followed by filtration of the desired salt and vacuum drying.[37] Then, 4.5 g (61 mmol) of 2-butanol and 2.3 g (20 mmol) of the formamidinium salt were stirred under reflux for 21 h. The mixture was cooled to room temperature, washed with 15 mL of Et_2O, and concentrated under vacuum. The residue was dissolved in 2 mL of MeOH and chromatographed over silica gel with 1.5:1 CH_2Cl_2/MeOH eluent. We obtained 1.29 g (8.4 mmol, 42%) of isouronium salt **8** as a highly hygroscopic, glassy solid (under vacuum), that fused to a slightly yellow oil in the atmosphere.

^{1}H NMR (DMSO-d_6): 0.84 (t, J = 7 Hz, 3 H, CH_2CH_3); 1.21 (d, J = 6 Hz, $CHCH_3$); 1.45-1.65 (m, 2 H, CH_2); 4.75-4.95 (m, 1 H, CH); 8.67 (br s, 4 H, $2N^+H_2$).

Anal. Calcd for $C_5H_{13}ClN_2O\cdot0.1H_2O$: C, 38.9; H, 8.62; N, 18.2; Cl, 23.0. Found: C, 38.4; H, 8.56; N, 18.5; Cl, 23.4.

Conversions of (*S*)-2-butanol to (*S*)-**8** were carried out analogously. Detailed descriptions of the optical rotations of these materials appear in the text.

3-(2-Butoxy)-3-chlorodiazirine (9). The Graham oxidation[18] was carried out on 1.29 g (8.4 mmol) of isouronium salt **8**. The salt was dissolved in 5 mL of DMSO; then, 15 mL of pentane and 0.1 g (2.4 mmol) of LiCl were added. The mixture was stirred and cooled to 5 °C while 220 mL of 12.5% aqueous NaOCl was added dropwise. The reaction temperature was kept at 10-13 °C during the addition. Stirring was continued for 20 min at 13 °C after addition of the hypochlorite. Then, 150 mL of ice water was added, the pentane layer was separated, the aqueous layer was extracted with 10 mL of pentane, and the organic extracts were combined. The resulting pentane solution of **9** was washed with 50 mL of brine and then dried over $CaCl_2$. Higher boiling solvents (MeCN, 1-butanol) could then be added and pentane removed at 0 °C under aspirator vacuum, to afford solutions of diazirine **9** in other solvents. The UV and NMR spectra of **9** are described above; it was too unstable to chromatograph. (*S*)-**9** was prepared from (*S*)-**8** in the same way.

(*S*)-2-Chlorobutane (12). (*R*)-(-)-2-Butanol (Aldrich, $[\alpha]^{23}_D$ -12.8° (neat)), 6.2 mL (5.0 g, 67.5 mmol), and 4.6 mL of dichlorophenylphosphine (Aldrich, 6.1 g, 34 mmol) were combined and stirred for 1 h at 0 °C. The product was isolated by vacuum distillation at 0.5 Torr from the solid residue, followed by conventional distillation (bp 68 °C). We obtained 1.75 g (19 mmol, 56% based on phosphine) of (*S*)-2-chlorobutane, $[\alpha]^{22}_D$ +32.0.[22]

(*S*)-2-Butyl 1-Butyl Ether (13). To a cooled (~10 °C) suspension of 1.68 g (70 mmol) of NaH in 20 mL of THF was added 5.2 mL (6.6 g, 48 mmol) of 1-bromobutane. Then, 5.6 mL (4.5 g, 61 mmol) of (*S*)-2-butanol (Aldrich, $[\alpha]^{24}_D$ +12.2° (neat)) was added dropwise with stirring. The mixture was warmed to room temperature and then stirred under reflux for 16 h. The product mixture was then cooled in an ice bath, and 25 mL of water was slowly added. The organic phase was separated, combined with 2 × 10 mL ether extracts of the aqueous phase, washed with water, and dried over $CaCl_2$. Volatiles were stripped at <18 °C using an aspirator vacuum, and the residue was distilled over a 20-cm Vigreux column. The desired **13** was collected at 121-122 °C. We obtained 5.5 g (42 mmol, 88% based on bromobutane) of **13** $[\alpha]^{24}_D$ +16.5° (c = 20, 1-butanol). Corrected for the optical purity of the initial 2-butanol[17] (87.8%), the specific rotation of optically pure **13** should be 18.8° in 1-butanol.

NMR (DMSO-d_6): 0.75-0.9 (m, 6 H, 2 superimposed CH_2CH_3); 0.98 (d, J = 6 Hz, $CHCH_3$); 1.2-1.5 (m, 6 H, $3CH_2$); 3.05-3.3 (m, 2 H, C*OCH_2); 3.3-3.45 (m, 1 H, CH).

Anal. Calcd for $C_8H_{18}O$: C, 73.8; H, 13.9. Found: C, 74.0; H, 13.9.

Decomposition Reactions of 9. The conditions and analyses for the decompositions of **9** in acetonitrile or 1-butanol are described in detail in the Results and Discussion. Both solvents were Aldrich, spectroscopic grade. In addition, the acetonitrile was dried over P_2O_5 and distilled prior to use. All polarimetric work is also presented above, the results are collected in Table I.

Acknowledgment. We are grateful to the National Science Foundation and to the National Science Foundation-Polish Academy of Sciences Cooperative Program (P.B.) for financial support. We thank Drs. Joanna Włostowska and Tadeusz Zdrojewski for initial synthetic studies of **8**.

(37) The precise description is given in Example 5 of ref 15.

Main Chain and Side Chain Chiral Methylated Somatostatin Analogs: Syntheses and Conformational Analyses

Ziwei Huang,[†] Ya-Bo He,[†] Karen Raynor,[‡] Melanie Tallent,[‡] Terry Reisine,[‡] and Murray Goodman*,[†]

Contribution from the Department of Chemistry, 0343, University of California, San Diego, La Jolla, California 92093, and Department of Pharmacology, University of Pennsylvania, Philadelphia, Pennsylvania 19104. *Received June 30, 1992*

Abstract: We have developed an integrated approach for investigating the "bioactive conformations" of the main chain and side chains for the somatostatin analog c[Pro^6-Phe^7-D-Trp^8-Lys^9-Thr^{10}-Phe^{11}]. A series of analogs have been synthesized incorporating α-methylated and β-methylated residues at positions 7, 8, and 11. These analogs display dramatic differences in in vitro binding affinities for somatostatin receptors. Using 500-MHz ^{1}H NMR and computer simulations, we have assessed the effect of main chain and side chain chiral methylations on the overall structure. The analyses of the changes of side chain topologies and subsequent binding affinities in the β-methylated analogs have provided definitive evidence about the "bioactive conformation" of the side chains of Phe^7, Trp^8, and Phe^{11}. The analyses of the α-methylated analogs have defined a "folded" feature for the peptide backbone. From this study, we have proposed a binding "pocket" for somatostatin analogs which consists of the side chains of Trp^8 and Lys^9, the peptide backbone, and the side chain of Phe^{11} in a "folded" topochemical array. In this "folded" conformation, the Trp^8 side chain assumes the trans rotamer, while the Lys^9 side chain assumes the gauche-rotamer, thus allowing a close proximity between these two side chains. The Phe^{11} side chain assumes the trans rotamer. The peptide backbone adopts a β II' turn about Trp^8-Lys^9 and a β VI turn about Phe^{11}-Pro^6. The overall structure is folded about Phe^7 and Thr^{10} residues assuming a C_7 conformation for their ϕ and ψ torsions. This model should have important implications on the future design of peptide or nonpeptide ligands with somatostatin-like activities.

Introduction

Initially, somatostatin was known for its ability to inhibit the release of growth hormone.[1] Since then, somatostatin has also been shown to suppress the release of many other bioactive molecules, including glucagon, insulin, gastrin, and secretin.[2-5]

* To whom correspondence should be addressed.
[†] University of California.
[‡] University of Pennsylvania.

(1) Brazeau, P.; Vale, W.; Burgus, R.; Ling, N.; Bucher, M.; Rivier, J.; Guillemin, R. *Science* **1973**, *179*, 77-79.
(2) Koerker, D. J.; Harker, L. A.; Goodner, C. J. *N. Engl. J. Med.* **1975**, *293*, 476-479.

0002-7863/92/1514-9390$03.00/0

In addition, because of its distribution in various brain regions and the spinal cord, it has been suggested that somatostatin plays a role in neural transmission.[6]

The possible clinical applications of somatostatin have made it the subject of intense structure–bioactivity studies. This led to the synthesis of the cyclic hexapeptide analog of somatostatin c[Pro^6-Phe^7-D-Trp^8-Lys^9-Thr^{10}-Phe^{11}] (**I**) by Veber and co-workers (the superscript numbers refer to the location of the residues in native somatostatin).[7] This molecule shows higher biological activity than native somatostatin in inhibiting the release of growth hormone, insulin, and glucagon. From NMR studies, Veber proposed a β II′ turn around Trp^8-Lys^9 and a β VI turn around Phe^{11}-Pro^6 with a cis amide bond.[8] Conformational studies of this cyclic hexapeptide analog **I** of somatostatin and subsequent active analogs by Kessler and Van Binst and co-workers confirmed the β II′ turn about D-Trp^8 and Lys^9 and the β VI turn with a cis amide bond about Phe^{11} and Pro^6, the so-called bridging region.[9,10] Applying retro-inverso approaches,[11] Goodman and co-workers synthesized cyclic hexapeptide analogs with retro-inverso modifications.[12] These studies suggested that the backbone of this peptide contributed little to receptor binding. Recently, Hirschmann, Nicoloau, and co-workers designed a peptidomimetic of somatostatin employing a β-D-glucose derivative.[13] They suggested that the peptide backbone was not required for receptor binding but served as a scaffold for supporting the key side chain groups of Phe^7, Trp^8, Lys^9, and Phe^{11} in a proper spatial arrangement.

Veber, Nutt, and co-workers carried out many studies to investigate the side chain conformations of somatostatin analogs.[14-16] Based on the changes of chemical shifts of some key protons, they suggested that the close proximity of Trp^8 and Lys^9 side chains and the trans rotamers for both Phe^7 and Phe^{11} side chains were important for bioactivity. Since the most important conformational parameter for the side chain conformation is the torsional angle χ_1 about the C^α–C^β bond, we applied a different approach of side chain rotamer analyses for studying the side chain conformation of the cyclic hexapeptide **I**. As will be discussed in a later section of this paper, we determined side chain rotamer populations and found that only the Lys^9 side chain displayed a highly constrained conformation with a predominant population on the gauche− (g^-) rotamer. The greatly constrained side chain conformation observed for the Lys^9 residue supports Veber's model.[8] However, three other important side chains of Phe^7, Trp^8, and Phe^{11} displayed a large degree of flexibility. The flexible nature of these aromatic side chains does not provide direct evidence about the side chain rotameric conformations required for binding to a somatostatin receptor. Therefore, further studies utilizing constraints on side chain conformations are of great importance because (1) the constrained side chain can provide more direct information on the possible "bioactive conformations" when bound to a receptor and (2) by constraining the side chain to prefer a "bioactive conformation", analogs of somatostatin with higher potencies and selectivities can be obtained.

Table I. Binding Constants for Somatostatin Analogs

	analog	IC_{50} (nM)
I	c[Pro-Phe-D-Trp-Lys-Thr-Phe]	1
II	c[Pro-(2*S*,3*S*)-β-MePhe-D-Trp-Lys-Thr-Phe]	1
III	c[Pro-(2*S*,3*R*)-β-MePhe-D-Trp-Lys-Thr-Phe]	1
IV	c[Pro-Phg-D-Trp-Lys-Thr-Phe]	15
V	c[Pro-Phe-(2*R*,3*S*)-β-MeTrp-Lys-Thr-Phe]	<1
VI	c[Pro-Phe-(2*R*,3*R*)-β-MeTrp-Lys-Thr-Phe]	>1000
VII	c[Pro-Phe-(2*S*,3*R*)-β-MeTrp-Lys-Thr-Phe]	10
VIII	c[Pro-Phe-(2*S*,3*S*)-β-MeTrp-Lys-Thr-Phe]	>1000
IX	c[Pro-Phe-D-Trp-Lys-Thr-(2*S*,3*S*)-β-MePhe]	50
X	c[Pro-Phe-D-Trp-Lys-Thr-(2*S*,3*R*)-β-MePhe]	>1000
XI	c[Pro-Phe-D-Trp-Lys-Thr-(2*R*,3*S*)-β-MePhe]	>1000
XII	c[Pro-Phe-D-Trp-Lys-Thr-(2*R*,3*R*)-β-MePhe]	>1000
XIII	c[Pro-(*S*)-α-MePhe-D-Trp-Lys-Thr-Phe]	>1000
XIV	c[Pro-(*R*)-α-MePhe-D-Trp-Lys-Thr-Phe]	>1000

We have developed an approach utilizing side chain chiral constraints to probe the side chain topologies of somatostatin analogs. Peptidomimetics β-methylphenylalanine (β-MePhe) and β-methyltryptophan (β-MeTrp) were designed and used to replace Phe and Trp residues at positions 7, 8, and 11 in the cyclic hexapeptide **I**. Our design rationale for these β-methylated residues is based on two considerations: (1) a topological effect of the β-methyl group which reduces the flexibility of the side chain and specifically constrains the side chain to prefer a particular rotamer and (2) a chiral effect of the β-methyl group which may have different steric effects on a receptor surface depending on the chiralities of the C^β atom. For phenylalanine and tryptophan, results from X-ray analyses and energy calculations indicated that the gauche+ (g^+) rotamer around the side chain χ_1 torsion is the least stable (highest energy) conformation and that the g^- and trans rotamers are nearly equivalent.[17] As for β-methylated phenylalanine and tryptophan, because of the steric effect introduced by a β-methyl group, the population equilibrium among the three rotameric states for the side chains is shifted toward a particular rotamer depending on the chiralities at the C^β atom. Hruby and co-workers synthesized cyclic enkephalin analogs utilizing β-MePhe.[18] They suggested that the side chain of the (2*S*,3*R*)-β-MePhe isomer may be constrained to the trans rotamer, while the side chain of the (2*S*,3*S*)-β-MePhe isomer may be constrained to the g^- rotamer. Therefore, we anticipated that the incorporation of these β-methylated residues should both modify the side chain topology that interacts with the receptor and, subsequently, affect binding affinity. In this manner, important insight into the "bioactive side chain conformation" may be obtained by correlating changes of the side chain topology with

(3) Gerich, J. E.; Lovinger, R.; Grodsky, G. M. *Endocrinology* **1975**, *96*, 749–754.
(4) Johansson, C.; Wisen, O.; Efendic, S.; Uvnas-Wallensten, K. *Digestion* **1981**, *22*, 126–137.
(5) Iverson, L. L. *Ann. Rev. Pharmacol. Toxicol.* **1983**, *23*, 1–27.
(6) Seybold, V. S.; Hylden, J. L. K.; Wilcox, G. L. *Peptides* **1982**, *3*, 49–54.
(7) Veber, D. F.; Freidinger, R. M.; Perlow, D. S.; Paleveda, W. J., Jr.; Holly, F. W.; Strachan, R. G.; Nutt, R. F.; Arison, B. J.; Homnick, C.; Randall, W. C.; Glitzer, M. S.; Saperstein, R.; Hirschmann, R. *Nature* **1981**, *292*, 55–58.
(8) Veber, D. F. In *Peptides, Synthesis, Structure and Function, Proceedings of the Seventh American Peptide Symposium*; Rich, D. H., Gross, V. J., Eds.; Pierce Chemical Co.: Rockford, IL, 1981; pp 685–694.
(9) Kessler, H.; Bernd, M.; Kogler, H.; Zarbock, J.; Sorensen, O. W.; Bodenhausen, G.; Ernst, R. R. *J. Am. Chem. Soc.* **1983**, *105*, 6944–6952.
(10) Elseviers, M.; Jaspers, H.; Delaet, N.; De Vadder, S.; Pepermans, H.; Tourwé, D.; Van Binst, G. In *Peptides, Chemistry, Structure and Biology, Proceedings of the Eleventh American Peptide Symposium*; Rivier, J. E., Marshall, G. R., Eds.; ESCOM: Leiden, 1989; pp 198–200.
(11) Goodman, M.; Chorev, M. *Acc. Chem. Res.* **1979**, *12*, 1.
(12) (a) Pattaroni, C.; Lucietto, P.; Goodman, M.; Yamamoto, G.; Vale, W.; Moroder, L.; Gazerro, L.; Göhring, W.; Schmied, B.; Wünsch, E. *Int. J. Pept. Protein Res.* **1990**, *36*, 401–417. (b) Mierke, D. F.; Pattaroni, C.; Delaet, N.; Toy, A.; Goodman, M.; Tancredi, T.; Motta, A.; Temussi, P. A.; Moroder, L.; Bovermann, G.; Wünsch, E. *Int. J. Pept. Protein Res.* **1990**, *36*, 418–432. (c) A cyclic hexapeptide c[*S*-mAla-Phe-D-Trp-Lys-Thr-gPhe] containing a retro-inverso modification at the bridging region displays a high affinity for the somatostatin receptor: unpublished results from this laboratory.
(13) Nicoloau, K. C.; Salvino, J. M.; Raynor, K.; Pietranico, S.; Reisine, T.; Freidinger, R. M.; Hirschmann, R. In *Peptides: Chemistry, Structure and Biology, Proceedings of the Eleventh American Peptide Symposium*; Rivier, J. E., Marshall, G. R., Eds.; ESCOM: Leiden, 1990; pp 881–884.
(14) Nutt, R. F.; Saperstein, R.; Veber, D. F. In *Peptides: Structure and Function, Proceedings of the Eighth American Peptide Symposium*; Hruby, V., Rich, D., Eds.; Pierce Chemical Co.: Rockford, IL, 1983; pp 345–348.
(15) Nutt, R. F.; Curley, P. E.; Pitzenberger, S. M.; Freidinger, R. M.; Saperstein, R.; Veber, D. F. In *Peptides: Structure and Function, Proceedings of the Ninth American Peptide Symposium*; Deber, C. M., Hruby, V., Kopple, K. D., Eds.; Pierce Chemical Co.: Rockford, IL, 1985; pp 441–444.
(16) Nutt, R. F.; Colton, C. D.; Saperstein, R.; Veber, D. F. In *Somatostatin*; Reichlin, S., Ed.; Plenum Publishing Corporation: New York, 1987; pp 83–88.
(17) (a) Bhat, T. N.; Sasisekharan, V.; Vijayan, M. *Int. J. Pept. Protein Res.* **1979**, *13*, 170–184. (b) Chuman, H.; Momany, F. A. *Int. J. Pept. Protein Res.* **1984**, *24*, 249–266.
(18) Hruby, V. J.; Toth, G.; Gehrig, C. A.; Kao, L. F.; Knapp, R.; Lui, G. K.; Yamamura, H. I.; Kramer, T. H.; Davis, P.; Burks, T. F. *J. Med. Chem.* **1991**, *34*, 1823–1830.

changes in binding potencies. Also, because of the diastereoisotopic nature of C^{β} hydrogens, β-methyl substitution will project the methyl group into different spatial zones, thus interacting differently with the receptor. This may provide valuable information on a receptor surface.

In this paper, we report the syntheses, binding studies, and conformational analyses of a series of cyclic hexapeptide analogs of somatostatin containing β-MePhe and β-MeTrp. These β-methylated analogs show widely different binding potencies at the somatostatin receptor (Table I). For instance, the (2*R*,3*S*)-β-MeTrp[8] analog **V** is more active than the parent compound **I** in binding, while the (2*R*,3*R*)-β-MeTrp[8] analog **VI** is totally inactive, a difference of more than 1000-fold on binding constants. Also, among the four diastereomers of β-MePhe[11], only the (2*S*,3*S*) analog **IX** displays high binding potency, while the other three analogs **X–XII** are inactive. The dramatic changes in binding suggest critical topochemical requirements for these side chain groups. Using high resolution one-dimensional and two-dimensional ^{1}H NMR experiments and computer simulations, we have carried out conformational analyses for these β-methylated analogs in order to assess systematically the effect of chiral variations on the overall structure. Such analyses have revealed two types of overall topologies for active somatostatin analogs. Further syntheses and conformational analyses of two analogs containing α-methylphenylalanine (α-MePhe) at position 7 suggest a "folded" topochemical array of the main chain and side chains for somatostatin analogs when bound to receptors. This study has demonstrated an integrated approach utilizing α- and β-methyl chiral substitutions for specific constraints of main chain and side chain conformations.

Synthesis

The diastereomers of β-methylphenylalanine (H-β-MePhe-OH, **1**) were prepared by condensation of α-methylbenzyl bromide with acetamidomalonate, followed by hydrolysis and decarboxylation of the condensate.[19] The optically pure compounds H-(2*S*,3*R*)- and H-(2*S*,3*S*)-β-MePhe-OH (**1a** and **1b**) were prepared by a modified method utilizing an enzymatic hydrolysis of *N*-(trifluoroacetyl)-β-MePhe-OH,[20] followed by HPLC separation. The absolute chiralities of **1a** and **1b** were determined by comparison of ^{1}H NMR and the optical rotation data with reported data.[19] Boc-(2*S*,3*R*)-β-MePhe-OH (**2a**) and Boc-(2*S*,3*S*)-β-MePhe-OH (**2b**) were prepared by the reaction of **1a** and **1b** with di-*tert*-butyl carbonate [$(Boc)_2O$] in the presence of triethylamine, respectively.[20] For β-methyltryptophan (**3**), the threo isomers H-(2*R*,3*S* + 2*S*,3*R*)-β-MeTrp-OH (**3a**) and the erythro isomers H-(2*R*,3*R* + 2*S*,3*S*)-β-MeTrp-OH (**3b**) were prepared according to the method of Synder.[21] Previously the threo isomers **3a** were distinguished from erythro isomers **3b** on the basis of the proton coupling constants.[22] In our present work, X-ray diffraction analysis of a single crystal, previously assigned as the threo isomers of *N*-acetyl-β-MeTrp-OH obtained from recrystallization in acetone–water, was performed. The results from the X-ray study confirmed the initial assignment. The corresponding Boc-(2*R*,3*S* + 2*S*,3*R*)-β-MeTrp-OH (**4a**) and Boc-(2*R*,3*R* + 2*S*,3*S*)-β-MeTrp-OH (**4b**) were prepared from the reaction of **3a** and **3b** with 2-(*tert*-butoxycarbonyloximido)-2-phenylacetonitrile (BocON) in the presence of triethylamine, respectively. Synthesis of racemic α-methylphenylalanine (H-α-MePhe-OH, **5**) was carried out according to literature procedure.[23] The amino acid **5** was converted to the methyl ester, which, in turn, coupled with Boc-Pro-OH to form Boc-Pro-(*SR*)-α-MePhe-OMe (**6**). Hydrolysis of the methyl ester provided Boc-Pro-(*SR*)-α-MePhe-OH (**7**). This approach was employed because of the poor yield obtained when an amino protecting group, such as Boc, was initially applied. The dipeptide **7** was used for segment coupling in the peptide synthesis.

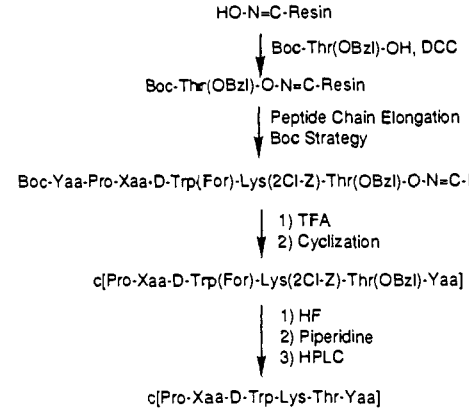

II Xaa: (2*S*,3*S*)-β-MePhe, Yaa : Phe; III Xaa: (2*S*,3*R*)-β-MePhe, Yaa: Phe;
IV Xaa: Phg, Yaa: Phe; IX Xaa: Phe, Yaa: (2*S*,3*S*)-β-MePhe;
X Xaa: Phe, Yaa: (2*S*,3*R*)-β-MePhe; XI Xaa: Phe, Yaa: (2*R*,3*S*)-β-MePhe;
XII Xaa: Phe, Yaa: (2*R*,3*R*)-β-MePhe; XIII Xaa: *S*-α-MePhe, Yaa: Phe;
XIV Xaa: *R*-α-MePhe, Yaa: Phe

Figure 1. Scheme for the syntheses of the peptides **II–IV** and **IX–XIV** on oxime resin.

Cyclic hexapeptides c[Pro-(2*S*,3*S*)-β-MePhe-D-Trp-Lys-Thr-Phe] (**II**), c[Pro-(2*S*,3*R*)-β-MePhe-D-Trp-Lys-Thr-Phe] (**III**), c[Pro-Phg-D-Trp-Lys-Thr-Phe] (**IV**) (Phg: phenylglycine), c-[Pro-Phe-D-Trp-Lys-Thr-(2*S*,3*S*)-β-MePhe] (**IX**), c[Pro-Phe-D-Trp-Lys-Thr-(2*S*,3*R*)-β-MePhe] (**X**), c[Pro-(*S*)-α-MePhe-D-Trp-Lys-Thr-Phe] (**XIII**), and c[Pro-(*R*)-α-MePhe-D-Trp-Lys-Thr-Phe] (**XIV**) were synthesized by solid-phase peptide synthesis methodology on *p*-nitrobenzophenone oxime resin. This approach is reported to possess an advantage in the syntheses of cyclic peptides, as it allows both the solid-phase assembly of the peptide chain and the subsequent intrachain cyclization and concomitant cleavage of the peptidyl–resin linkage to be performed in consecutive steps on the same support.[24] Syntheses were carried out starting from Boc-Thr(OBzl)-OH[25] linked to oxime resin. We utilized a low substitution level in order to minimize interchain side reactions during the cyclization step. Each peptide chain was then assembled by consecutive cleavage steps of Boc groups and addition of the *N*-Boc amino acids. After the last Boc group was removed from the N-terminal residue, the liberated amino group was allowed to react with the activated C-terminus attached to the resin, thereby releasing the side chain protected cyclic hexapeptide derivative. Hydrogenolysis of the peptides failed to deprotect completely 2Cl-Z and OBzl groups. Alternatively, HF cleavage was employed to remove successfully these protecting groups. Final deprotection of the formyl groups on tryptophan yielded the desired cyclic hexapeptides, which were separated and purified by preparative RP-HPLC (Figure 1). It is noted that the chiralities of the C^{α} atoms of α-MePhe in the peptides **XIII** and **XIV** were determined by NMR according to the procedure of Yamazaki and Goodman.[26]

(19) Kataoka, Y.; Seto, Y.; Yamamoto, M.; Yamada, T.; Kumata, S.; Watanabe, H. *Bull. Chem. Soc. Jpn.* **1976**, *49*, 1081–1084.
(20) Samanem, J.; Narindray, D.; Cash, T.; Brandeis, E.; Adams, W., Jr.; Yellin, T.; Eggleston, D.; Debrosse, C.; Regoli, D. *J. Med. Chem.* **1989**, *32*, 466–472.
(21) Synder, H. R.; Matteson, D. S. *J. Am. Chem. Soc.* **1957**, *79*, 2217–2221.
(22) (a) Turchin, K. F.; Preobrazhenskaya, M. N.; Savel'eva, L. A.; Belen'kaya, E. S.; Kostyuchenko, N. P.; Scheinker, Y. N.; Suvorov, N. N. *J. Org. Chem. USSR* **1971**, *7*, 1329–1334. (b) Spondlin, C.; Tamm, C. *Heterocycles* **1989**, *28*, 453–465.
(23) Stein, G. A.; Bronner, H. A.; Pfister, K., III *J. Am. Chem. Soc.* **1955**, *77*, 700–703.
(24) (a) Ösapay, G.; Taylor, J. W. *J. Am. Chem. Soc.* **1990**, *112*, 6046–6051. (b) Ösapay, G.; Profit, A.; Taylor, J. W. *Tetrahedron Lett.* **1990**, *31*, 6121–6124.
(25) Abbreviations used are those recommended by the IUPAC-IUB Commission: Bzl, benzyl; 2Cl-X, 2-chlorobenzyloxycarbonyl; Boc, *tert*-butyloxycarbonyl; For, formyl; Fmoc, 9-fluorenylmethyloxycarbonyl; DCC, dicyclohexylcarbodiimide; EDC, ethyl diisopropylcarbodiimide; HOBt, 1-hydroxybenzotriazole; BOP, (benzotriazol-1-yloxy)tris(dimethylamino)-phosphonium hexafluorophosphate; DPPA, diphenylphosphoryl azide; TFA, trifluoroacetic acid; DIEA, *N,N'*-diisopropylethylamine; DCM, dichloromethane.

Table II. Physical Properties and Analytical Data for Somatostatin Analogs II–XIV[a]

analog	yield[c] (%)	TLC R_f(B)	HPLC[b] t_R (min)	amino acid analysis	HR-FABMS m/z calcd	HR-FABMS m/z found
II	10	0.63	(36%) 22.8	Lys 1.00, Thr 0.95, Phe 1.09, Pro 1.00, Trp 1.09	821.4350 (M + H)$^+$	821.4327
III	18	0.62	(35%) 23.2	Lys 1.00, Thr 0.96, Phe 1.03, Pro 1.00, Trp 0.94	821.4350 (M + H)$^+$	821.4376
IV	8	0.59	(34%) 34.0	Lys 1.00, Thr 1.00, Phe 0.99, Pro 0.92, Trp 0.91	793.4037 (M + H)$^+$	793.4012
V	19	0.49	(35%) 29.1	Lys 0.89, Thr 0.92, Phe 2.00, Pro 0.97	821.4350 (M + H)$^+$	821.4395
VI	12	0.45	(35%) 29.5	Lys 1.03, Thr 0.89, Phe 2.00, Pro 1.02	821.4350 (M + H)$^+$	821.4363
VII	11	0.46	(35%) 22.4	Lys 1.03, Thr 0.94, Phe 2.00, Pro 1.02	821.4350 (M + H)$^+$	821.4370
VIII	16	0.42	(35%) 26.1	Lys 1.11, Thr 0.90, Phe 2.00, Pro 1.01	821.4350 (M + H)$^+$	821.4353
IX	6	0.66	(32%) 74.6	Lys 1.00, Thr 0.98, Phe 1.04, Pro 0.95, Trp 0.87	821.4350 (M + H)$^+$	821.4307
X	6	0.67	(32%) 56.1	Lys 1.00, Thr 1.00, Phe 1.08, Pro 0.97, Trp 0.85	821.4350 (M + H)$^+$	821.4368
XI	1	0.65	(32%) 70.7	Lys 1.00, Thr 1.00, Phe 1.08, Pro 0.96, Trp 0.88	843.4170 (M + Na)$^+$	843.4191
XII	1	0.65	(32%) 69.8	Lys 1.00, Thr 0.99, Phe 1.07, Pro 0.95, Trp 0.88	821.4350 (M + H)$^+$	821.4311
XIII	13	0.59	(34%) 32.2	Lys 1.00, Thr 0.93, Phe 1.10, Pro 0.93, Trp 0.82	821.4350 (M + H)$^+$	821.4321
XIV	3	0.60	(34%) 23.6	Lys 1.00, Thr 0.99, Phe 1.10, Pro 0.89, Trp 0.82	821.4350 (M + H)$^+$	821.4329

[a] Analytical data for the intermediate protected cyclic hexapeptides (for II–IV and IX–XIV) and linear hexapeptides (for V–VIII) are given in the supplementary material. [b] Vydac C_{18} proteins preparative column; eluent (X%) CH_3CN/H_2O with 0.1% TFA; flow rate 8 mL/min; detection at 215 nm. [c] Yield based on the starting Boc-Thr(OBzl)-resin.

Table III. Summary of the Backbone Interresidue NOEs Observed for Three Pairs of Diastereomers (II, III, V, VI, XI, and XII) Containing β-Methylation at Positions 7, 8, and 11, Respectively[a]

	β-MePhe^7		β-MeTrp^8		β-MePhe^{11}	
	2*S*,3*S*	2*S*,3*R*	(2*R*,3*S*)	2*R*,3*R*	2*R*,3*S*	2*R*,3*R*
NOE(Pro^{6}C$^\alpha$H-Phe^{7}NH)	–	m	–	–	–	–
NOE(Pro^{6}C$^\delta$H-Phe^{7}NH)	–	m	–	m	–	–
NOE(Phe^{7}C$^\alpha$H-Trp^{8}NH)	s	s	s	s	s	s
NOE(Trp^{8}C$^\alpha$H-Lys^{9}NH)	s	s	s	s	s	s
NOE(Lys^{9}NH-Thr^{10}NH)	m	m	m	m	w	w
NOE(Thr^{10} C$^\alpha$H-Phe^{11} NH)	s	s	s	s	m	m
NOE(Phe^{11}C$^\alpha$H-Pro^{6}C$^\alpha$H)	s	s	s	s	–	–
NOE(Phe^{11}C$^\alpha$H-Pro^{6}C$^\delta$H)	–	–	–	–	s	s

[a] The observed NOEs are qualitatively classified according to their intensities: s, strong; m, medium; w, weak; –, absent.

It should also be pointed out that during the syntheses of peptides **IX** and **X**, a small amount of the diastereomers c[Pro-Phe-D-Trp-Lys-Thr-(2*R*,3*S*)-β-MePhe] (**XI**) and c[Pro-Phe-D-Trp-Lys-Thr-(2*R*,3*R*)-β-MePhe] (**XII**) were also obtained from HPLC separation. For the analogs **XI** and **XII** the chirality of the C$^\alpha$ atom of β-MePhe was determined by NMR.[26] The chirality assignment for the C$^\beta$ atom of β-MePhe was made arbitrarily because the C$^\beta$ atom could not be assigned unambiguously by NMR. Since the two analogs **XI** and **XII** do not contain the required cis amide bond at the bridging region and have very low binding affinities, the present study is focused on other β-methylated analogs which contain a cis amide bond at the bridging region.

Cyclic hexapeptides c[Pro-Phe-(2*R*,3*S*)-β-MeTrp-Lys-Thr-Phe] (**V**), c[Pro-Phe-(2*R*,3*R*)-β-MeTrp-Lys-Thr-Phe] (**VI**), c[Pro-Phe-(2*S*,3*R*)-β-MeTrp-Lys-Thr-Phe] (**VII**), and c[Pro-Phe-(2*S*,3*S*)-β-MeTrp-Lys-Thr-Phe] (**VIII**) were synthesized on Merrifield resin, followed by cyclization in solution. After the linear hexapeptide chains were assembled, the peptides were cleaved by HF from the resin, with concomitant removal of Boc and OBzl groups. The separation of diastereomers of the linear hexapeptides was carried out by RP-HPLC. The cyclization of each compound was performed in DMF using DPPA as a coupling reagent. The resulting peptides were treated with piperidine to remove Fmoc groups from lysine, and the final products were purified by RP-HPLC. Since the threo (**4a**) as well as erythro (**4b**) isomers of Boc-β-MeTrp-OH were used in the syntheses instead of optically pure isomers, the absolute configuration of the C$^\alpha$ atom on the β-MeTrp residue in each final product was determined by NMR.[26] The absolute configuration of the C$^\beta$ atom could then be simply deduced as the relative configuration between C$^\alpha$ and C$^\beta$ atoms was previously established. Thus, the chiralities of the C$^\alpha$ and C$^\beta$ atoms on the β-MeTrp residues in the final products **V–VIII** were fully assigned.

Physical properties and analytic data of the target peptides **II–XIV** are listed in Table II.

(26) Yamazaki, T.; Goodman, M. *Chirality* **1991**, *3*, 1–9.

Results

The β-methylated and α-methylated analogs were measured for specific binding to the somatostatin receptor, and their potencies are presented in Table I. The results from binding and conformational studies for c[Pro-Phe-D-Trp-Lys-Thr-Phe] (I) synthesized by Veber and co-workers[7] are also reported for comparison (compound I will be referred to as the parent compound hereafter). As shown in Table I, these β-methylated analogs display widely different binding affinities. The molecules which are high affinity binders act as agonists since they inhibit cyclic AMP formation to the same extent as somatostatin. The other molecules that bind with much lower affinity also inhibit cyclic AMP formation and, therefore, must be very weak agonists.

The NMR data, including NOEs, $J_{NH-H\alpha}$ and $J_{H\alpha\beta}$ vicinal coupling constants, temperature coefficients of amide protons, and changes in chemical shifts, were used to analyze main chain and side chain conformational preferences. Table III shows some of the interresidue NOEs observed for three representative pairs of diastereomers containing β-methylated residues at positions 7, 8, and 11. These NOEs provide the most important information about backbone conformations. Further information about backbone conformations was derived from vicinal coupling constants $J_{NH-H\alpha}$, from which the torsion ϕ was calculated using a Karplus-type equation.[27,28] The vicinal coupling constants $J_{NH-H\alpha}$ and estimated ϕ torsions are given in Table IV for the β-MeTrp^8 diastereomers V–VIII. Temperature coefficients for the amide protons also provide information on backbone conformations by indicating solvent shielding or hydrogen bonding. As shown in Table V, the Thr^{10} NH proton displays small temperature coefficients for all analogs, which gives an indication of its involvement in intramolecular hydrogen bonding.

As for the side chain conformations, vicinal coupling constants $J_{H\alpha\beta}$ offer the most important information on side chain torsions

(27) Bystrov, V. F.; Ivanov, V. T.; Portnova, S. L.; Balashova, T. A.; Ovchinnikov, Y. A. *Tetrahedron* **1973**, *29*, 873–877.

(28) Cung, M. T.; Marraud, M.; Neel, J. *Macromolecules* **1974**, *7*, 606–613.

Table IV. $^3J_{NH-H\alpha}$ Coupling Constants and Calculated ϕ Values for Somatostatin Analogs V–VIII Containing β-MeTrp at Position 8

	(2R,3S)-β-MeTrp		(2R,3R)-β-MeTrp		(2S,3R)-β-MeTrp		(2S,3S)-β-MeTrp	
residue	$J_{NH-H\alpha}$[a]/Hz	ϕ[b]/deg	$J_{NH-H\alpha}$[a]/Hz	ϕ[b]/deg	$J_{NH-H\alpha}$[a]/Hz	ϕ[b]/deg	$J_{NH-H\alpha}$[a]/Hz	ϕ[b]/deg
Phe[7]	6.02	90 (60)	5.19	96 (76)	9.45		9.24	
		30		24 (44)				
		−161 (−167)		−166 (−171)		−134 (−147)		−137 (−148)
		−79 (−73)		−74 (−69)		−106 (−93)		−103 (−92)
β-MeTrp[8]	8.16	147 (155)	8.54	144 (153)	5.37	95 (72)	5.16	96 (76)
		93 (85)		96 (87)		25 (48)		24 (44)
		(−60)		(−60)		−165 (−170)		−166 (−171)
						−75 (−70)		−74 (−69)
Lys[9]	7.09	79 (60)	6.96	81 (60)	7.52	74 (60)	7.73	70 (60)
		41		39		46		50
		−154 (−161)		−155 (−162)		−151 (−158)		−150 (−157)
		−86 (−79)		−85 (−78)		−89 (−81)		−90 (−82)
Thr[10]	7.52	74 (60)	6.90	81 (60)	7.52	74 (60)	7.95	64 (60)
		46		38		46		56
		−151 (−158)		−156 (−162)		−151 (−158)		−148 (−156)
		−89 (−81)		−84 (−78)		−89 (−81)		−92 (−84)
Phe[11]	4.52	101 (84)	5.98	90 (60)	0.00	150 (150)	0.00	150 (150)
		19 (36)		30				
		−170 (−175)		−161 (−167)		−30 (−30)		−30 (−30)
		−70 (−65)		−79 (−73)				

[a] $J_{NH-H\alpha}$ values are within ±0.5 Hz. [b] Values were calculated using $J_{NH-H\alpha} = A\cos^2|\phi \pm 60°| - B\cos|\phi \pm 60°| + C$ where + is for a D-configuration and − is for an L-configuration. (A, B, C) = (8.6, 1.0, 0.4) as proposed by Bystrov[27] for a chiral residue. Values calculated using (A, B, C) = (8.6, 2.9, 0.0) as proposed by Cung[28] were also included in parentheses.

Table V. Temperature Coefficients[a] of the Amide Protons of β-Methylated Somatostatin Analogs I–XII

	analog											
residue	I	II	III	IV	V	VI	VII	VIII	IX	X	XI	XII
Phe[7]	1.6	1.7	2.7	3.2	5.4	0.1	3.4	3.8	0.6	0.7	1.4	1.0
D-Trp[8]	5.1	6.3	3.8	5.5	6.0	6.8	2.8	4.0	4.5	4.3	5.5	5.7
Lys[9]	5.4	5.3	3.8	5.2	5.4	6.2	4.1	1.0	4.8	4.8	5.2	5.1
Thr[10]	0.3	0.0	0.4	−0.9	−0.7	−0.2	0.0	−0.1	0.1	−2.5	−0.2	−1.4
Phe[11]	2.8	3.4	3.5	4.0	4.8	2.8	5.9	5.8	1.7	1.8	6.6	7.8

[a] Values in −ppb/K.

Table VI. $^3J_{H\alpha\beta}$ Coupling Constants[a] and Calculated Side Chain Populations for $\chi_1{}^g$ for β-Methylated Somatostatin Analogs I–XII

		β-MePhe[7]			β-MeTrp[8]				β-MePhe[11]			
residue	parent	2S,3S	2S,3R	Phg[7]	2R,3S	2R,3R	2S,3R	2S,3S	2S,3S	2S,3R	2R,3S	2R,3R
Phe[7]	5.92, 5.90	8.22[b]	7.62[b]	c	7.52, 5.16	4.78, 4.30	3.86, 12.26	3.76, 12.79	5.62, 5.64	5.94, 5.94	5.05, 8.00	5.79, 6.68
f(g⁻)	0.23	0.45			0.16	0.07	0.84	0.90	0.20	0.23	0.43	0.30
f(t)	0.23		0.40		0.38	0.12	0.03	0.02	0.20	0.23	0.14	0.22
f(g⁺)	0.54				0.46	0.81	0.13	0.08	0.60	0.54	0.43	0.48
Trp[8]	8.10, 7.22	15.25[d]	8.63, 6.86	7.82, 8.03	10.53[b]	11.02[b]	7.52[b]	8.15[b]	6.83, 8.04	7.37, 8.19	5.89, 7.58	6.70, 8.01
f(g⁻)	0.20	0.21	0.19	0.16				0.45	0.24	0.18	0.38	0.27
f(t)	0.44		0.49	0.41	0.68		0.38		0.44	0.45	0.23	0.30
f(g⁺)	0.36		0.32	0.43		0.72			0.32	0.37	0.39	0.43
Lys[9]	4.00, 10.09	3.66, 9.28	3.54, 10.45	3.62, 9.64	3.49, 10.77	3.36, 11.86	15.04[d]	15.04[d]	2.81, 10.45	3.48, 10.88	e	4.01, 8.91
f(g⁻)	0.68	0.61	0.72	0.64	0.75	0.84			0.67	0.76		0.58
f(t)	0.13	0.10	0.08	0.09	0.08	0.07			0.02	0.08		0.13
f(g⁺)	0.19	0.29	0.20	0.27	0.17	0.09	0.10	0.10	0.31	0.16		0.29
Thr[10f]	4.42	4.34	4.65	4.22	4.52	3.52	7.30	7.09	3.82	3.70	3.79	3.56
f(g⁻)	0.17	0.16	0.19	0.15	0.18	0.08	0.43	0.41	0.11	0.10	0.11	0.09
Phe[11]	7.15, 8.40	16.23[d]	15.8[d]	15.26[d]	15.67[d]	15.49[d]	2.37, 10.53	0.54, 11.92	8.04[b]	9.41[b]	9.47[b]	10.25[b]
f(g⁻)	0.35						0.00	0.00	0.44			
f(t)	0.47						0.68	0.81		0.57	0.57	
f(g⁺)	0.18	0.11	0.16	0.21	0.17	0.18	0.32	0.19				0.65

[a] Values are in hertz. [b] Because β-methylated residues have a single β proton, only one rotamer can be estimated depending on the chiralities of the C^α and C^β atoms. [c] The χ_1 population calculations are not applicable to phenylglycine residue. [d] The reported value is for $J_{H\alpha\beta1} + J_{H\alpha\beta2}$. $J_{H\alpha\beta1}$ and $J_{H\alpha\beta2}$ were difficult to measure because of overlap. Analyzing the multiplicity of the α proton resonance and utilizing the $J_{NH-H\alpha}$ constant gives $J_{H\alpha\beta1} + J_{H\alpha\beta2}$. From this value, the population f(g^+) for an L-residue or f(g^-) for a D-residue may be calculated. [e] Due to excessive overlap, the coupling constants could not be measured. [f] Because Thr has a single β proton, only the f(g^-) population can be calculated while the f(t) and f(g^+) populations of χ_1 cannot be distinguished. [g] f(g^-), f(t), f(g^+) represents the fraction of the χ_1 population in the gauche−, trans, and gauche+ rotamers, respectively.

χ_1. Using a three-state model, where the energy minima associated with χ_1 are trans, g^-, and g^+, the populations in each of these states were calculated using Pachler's equations[29] for nonaromatic amino acid residues and Cung's equations[30] for aromatic residues, respectively (Table VI). The observed signals to their respective β-protons were assigned following a procedure described by Yamazaki and co-workers.[31] Changes in chemical shifts may provide additional indications about the relative locations of aromatic side

(29) Pachler, K. G. P. *Spectrochim. Acta* **1964**, *20*, 581–587.
(30) Cung, M. T.; Marraud, M. *Biopolymers* **1982**, *21*, 953–967.
(31) Yamazaki, T.; Pröbstl, A.; Schiller, P. W.; Goodman, M. *Int. J. Pept. Protein Res.* **1991**, *37*, 364–381.

Table VII. Chemical Shifts for Somatostatin Analogs V–VIII Containing β-MeTrp at Position 8

residue	resonance (δ in ppm)	β-MeTrp analog 2*R*,3*S*	2*R*,3*R*	2*S*,3*R*	2*S*,3*S*
Pro[6]	α	3.75	3.67	2.92	2.88
	β	1.08/1.75	1.26/1.65	0.58/1.53	0.54/1.51
	γ	1.36/1.53	1.30/1.49	0.39/1.25	0.31/1.22
	δ	3.15/3.26	3.04/3.18	2.91/3.06	2.88/3.03
Phe[7]	NH	7.42	6.73	8.75	8.76
	α	4.74	4.43	4.54	4.32
	β	2.89/2.97	2.27/2.68	2.99/3.44	2.94/3.18
β-Me-Trp[8]	NH	8.53	8.38	7.71	7.42
	α	4.45	4.72	4.30	4.23
	β	3.23	3.26	3.52	3.52
	β-Me	0.96	1.30	1.42	1.35
Lys[9]	NH	8.23	9.00	8.01	7.96
	α	3.39	4.05	3.74	4.06
	β	1.14/1.36	1.57/1.84	1.53/1.62	1.48/1.63
	γ	0.35	1.38	1.02	1.22
	δ	1.14	1.54	1.36	1.48
	ε	2.41	2.76	2.58	2.70
Thr[10]	NH	6.93	7.04	7.07	6.94
	α	4.13	4.15	4.24	4.26
	β	3.89	4.03	3.75	3.75
	γ	0.99	0.97	1.14	1.15
	OH	4.90	5.20	4.69	4.69
Phe[11]	NH	8.30	8.13	8.87	8.93
	α	4.25	4.21	4.18	4.17
	β	2.89/2.89	2.84/2.84	2.79/3.02	2.79/3.03

chains. For instance, the upfield shift of Lys[9] C$^{\gamma}$ protons may be explained by the shielding by the Trp[8] side chain, which is in close proximity with the Lys[9] side chain.[8] By comparing changes in chemical shifts between diastereomers of the β-methylated analogs and the parent compound **I**, we were able to obtain information about the preferred side chain rotamers for the modified residues. Table VII lists the chemical shifts observed for the representative β-MeTrp[8] diastereomers **V–VIII**.

Utilizing the information obtained from the NMR experiments described above, we have carried out conformational searches to find all possible conformations consistent with the NMR data. Results from conformational searches for these analogs are summarized in Table VIII.

Discussion

As indicated by the NMR results, the backbone conformations of the parent compound **I** are maintained in all of the β-methylated analogs except for those analogs in which the chirality changes at the C$^{\alpha}$ atom. For the D-Trp[8]-containing analogs **I–VI** and **IX–XII**, NOEs observed for Phe[7] C$^{\alpha}$H–D-Trp[8] NH, D-Trp[8] C$^{\alpha}$H–Lys[9] NH, and Lys[9] NH–Thr[10] NH, together with the measured $J_{NH-H\alpha}$ coupling constants of Trp[8] and Lys[9], suggests a β II′ turn around D-Trp[8]-Lys[9] region. The low temperature coefficient measured for the Thr[10] NH proton in these analogs is consistent with a hydrogen bond between Thr[10] NH and Phe[7] CO which stabilizes the β II′ turn. For the L-amino acid-containing (2*S*,3*R*)-(**VII**) and (2*S*,3*S*)-β-MeTrp[8] (**VIII**) analogs, a β I turn is expected because of the L-chirality of the residues at positions $i + 1$ and $i + 2$.[32,33] The β I turn is supported by the NOEs observed for Phe[7] C$^{\beta}$H–Trp[8] NH and Trp[8] C$^{\beta}$H–Lys[9] NH. The $J_{NH-H\alpha}$ coupling constants of Trp[8] and Lys[9] for (2*S*,3*R*)- (**VII**) and (2*S*,3*S*)-β-MeTrp[8] (**VIII**) analogs are also in agreement with the β I turn about Trp[8]-Lys[9]. As for the bridging region, the strong NOE between the C$^{\alpha}$ protons of Phe[11] and Pro[6] observed for the L-Phe[11]-containing analogs **I–X** indicates a β VI turn with a cis amide linking Phe[11] and Pro[6]. For the (2*R*,3*S*)- (**XI**) and (2*R*,3*R*)-β-MePhe[11] (**XII**) analogs which contain a D-Phe[11], the strong NOE for β-MePhe[11] C$^{\alpha}$H–Pro[6] C$^{\delta}$H and the lack of NOE for β-MePhe[11] C$^{\alpha}$H–Pro[6] C$^{\alpha}$H enable us to exclude the presence of a cis amide bond and suggest a trans amide bond at the bridging region. These results suggest that, unless the chirality changes at the C$^{\alpha}$ atoms, the side chain β-methylation has little effect on the backbone conformations of the parent cyclic hexapeptide **I**.

Table VIII. Summary of Possible Conformations Found for β-Methylated Somatostatin Analogs I–XII

		analog[a] I–V, VII, IX "folded"	"flat"	XI, XII DF1	DF2	DF3
topology[b]						
d_{7-8}/Å[c]		8.7	7.9	7.8	6.0	5.6
d_{7-9}/Å		10.7	10.8	10.8	11.5	10.0
d_{7-11}/Å		8.0	7.8	8.6	8.1	9.0
d_{8-9}/Å		4.4	4.3	4.3	8.2	7.0
d_{8-11}/Å		8.4	11.9	12.2	10.4	11.6
d_{9-11}/Å		9.3	12.1	12.0	9.8	9.4
torsion[d]						
Pro[6]	φ/deg	−74	−74	−68	−61	−52
	ψ/deg	−20	−37	−38	75	−58
Phe[7]	φ/deg	−74	−142	−147	62	−153
	ψ/deg	83	167	167	159	−179
	χ_1/deg	−54	−59	−60	−54	−56
	χ_2/deg	97	100	98	95	98
Trp[8]	φ/deg	69	88	74	66	94
	ψ/deg	−139	−141	−143	−143	−65
	χ_1/deg	178	180	177	58	58
	χ_2/deg	−86	−87	−88	−93	−100
Lys[9]	φ/deg	−62	−66	−64	−64	−167
	ψ/deg	−35	−23	−30	−39	−25
	χ_1/deg	−62	−62	−62	−176	66
	χ_2/deg	−179	−179	180	−179	−60
Thr[10]	φ/deg	−84	−142	−162	−75	−154
	ψ/deg	75	−176	161	168	152
	χ_1/deg	58	62	61	63	−57
Phe[11]	φ/deg	−49	−66	73	−58	70
	ψ/deg	139	144	−140	−58	−137
	χ_1/deg	−174	−177	−175	177	−54
	χ_2/deg	91	90	94	117	92
δE[d] (kcal mol^{-1})		0.089	0.000	0.000	5.961	6.429

[a] Analogs are divided into two groups based on their similar topologies: active analogs (**I–V, VII, IX**) and inactive analogs (**XI, XII**). Inactive analogs **VI, VIII**, and **X** are not included in this table, and their conformations are discussed in the text. [b] The topology refers to the three-dimensional topological relationships between the side chains of residues 7, 8, 9, and 11. As discussed in the text, these side chains are the key elements for receptor binding, while the peptide backbone serves as a scaffold to support a proper side chain arrangement. Therefore, we propose that the topology, instead of the torsion angle, can better define the topochemical arrays for active and inactive analogs. [c] d_{7-8} refers to the side chain–side chain distance between residues 7 and 8. The side chain–side chain distance is defined by the distance between the side chain C$^{\gamma}$ atoms. The distances for six side chain–side chain combinations of residues 7, 8, 9, and 11 are given. [d] Torsional angles and relative energies at dielectric = 80 are given for analogs **V** and **XI** representing active (**I–IV, VII, IX**) and inactive (**XII**) analogs, respectively.

The β-methylations have dramatic effects on the conformational preferences of the modified side chains. In the following sections we focus our discussion on the conformational effects of β-methyl chiral substitutions on the flexible side chain of Phe[7], D-Trp[8], and Phe[11] in the parent compound **I**. Analyses of the different conformational and biological profiles observed for these β-methylated analogs enabled us to derive the possible "bioactive conformations" for the side chains of Phe[7], D-Trp[8], and Phe[11], respectively. Among the four proposed binding side chains of Phe[7], D-Trp[8], Lys[9], and Phe[11], only the Lys[9] side chain was not subjected to the β-methylation in this investigation. As discussed above, this side chain displays a highly constrained conformation for the g^- rotamer in the parent compound **I**. A similar conformation is also observed for the Lys[9] side chain in other active analogs (**II–V, IX**, Table VI). These results were consistent with the "bioactive conformation" of this side chain as proposed by Veber.[8]

"Bioactive Conformation" of the Phe[7] Side Chain. As shown in Table I, the (2*S*,3*S*)- (**II**) and (2*S*,3*R*)-β-MePhe[7] (**III**) analogs

(32) Rose, G. D.; Gierash, L. M.; Smith, J. A. *Adv. Protein Chem.* **1985**, *37*.

(33) Arison, B. H.; Hirschmann, R.; Veber, D. F. *Bioorg. Chem.* **1978**, *7*, 447–451.

display equal potencies in binding. Even though little perturbation of the backbone conformation is observed for these two β-methylated analogs, they display different side chain conformational preferences at the modified residue. As shown in Table VI, the side chain rotamer populations for the unmodified residues show little change between these two analogs and the parent compound (I). However, the population of g^- and trans rotamers for the β-MePhe[7] side chain is almost doubled in the 2S,3S (II) and 2S,3R (III) analogs, respectively. These results support our hypothesis that the side chain of the β-methylated residue is constrained to prefer a particular rotamer depending on the chirality of the C^β atom. The equal binding potencies shown by these two analogs, despite the differences in their side chain rotameric conformations at position 7, indicate that binding affinity is rather insensitive to the changes of side chain conformation at position 7. This is inconsistent with Veber's model for the Phe[7] side chain in which the trans rotamer was suggested to be important for bioactivity.[16] Therefore, we hypothesize that only the aromatic group at position 7 is important for binding activity, not its exact topochemistry. To examine this possibility, we designed and synthesized an analog (IV) incorporating a Phg residue at position 7. This analog retains an aromatic group at position 7 while its rotation around the C^α–C^β bond is eliminated. The high binding affinity shown by the Phg[7] analog IV fully supports our hypothesis.

"Bioactive Conformation" of the Trp[8] Side Chain. The side chain of β-MeTrp[8] is highly constrained to the trans and g^+ rotamers in the (2R,3S)- (V) and (2R,3R)-β-MeTrp[8] (VI) analogs, respectively. As shown in Table VI, the parent compound I shows a large degree of flexibility at the Trp[8] side chain. This lack of a highly preferred side chain rotamer for residue 8 does not provide convincing evidence about its "bioactive rotamer", even though the trans rotamer was proposed before to be important for bioactivity.[8] By substituting the C^β hydrogen with a methyl group, we were able to reduce the flexibility of the Trp[8] side chain substantially and specifically constrain this side chain to the trans and g^+ rotamers. Again, this strongly supports our hypothesis that different constrained side chain rotamers can be obtained by utilizing the β-methyl chiral substitution approach. The (2R,3S)-β-MeTrp[8] analog V has a higher binding potency than the parent compound I, while the (2R,3R)-β-MeTrp[8] analog VI has extremely low potency. Because similar backbone conformations were observed between these two analogs (V and VI) and the parent compound I as discussed above, the change of binding potency may be best explained by the change of side chain rotamer preference at residue 8. The substantial increase in the trans rotamer population of the β-MeTrp[8] side chain and resulting enhanced binding affinity observed in analog V provided direct evidence about the trans rotamer for the Trp[8] side chain as the "bioactive rotamer".

The changes of chemical shifts between the (2R,3S)- (V) and (2R,3R)-β-MeTrp[8] (VI) analogs and the parent compound I also provided additional evidence about the different side chain rotameric conformations of β-MeTrp[8] residue. As shown in Table VII, it is most noteworthy that the Lys[9] side chain C^γ protons are shifted significantly upfield to 0.35 ppm in the active (2R,3S)-β-MeTrp[8] analog V. This may be explained by the shielding effect of the indole ring in close proximity with the Lys[9] side chain, because the β-MeTrp[8] side chain greatly prefers the trans rotameric conformation. Meanwhile, the downfield shifting observed for the Lys[9] C^γ protons in the inactive (2R,3R)-β-MeTrp[8] analog VI is consistent with the deshielding effect caused by the β-MeTrp[8] side chain, which moves away from the Lys[9] side chain and takes a predominant g^+ rotameric conformation. Noticeable changes of chemical shifts were also observed for protons in residues 7 and 9 in which the chemical shifts of these protons displayed different trends for the active (V) and inactive (VI) analogs. The difference in the chemical shifts of protons in Phe[7] and Lys[9] adjacent to the modified β-MeTrp[8] may be explained by the shielding and deshielding effects from the β-MeTrp[8] side chain in different spatial orientations as described above.

As for the (2S,3R)- (VII) and (2S,3S)-β-MeTrp[8] (VIII) analogs, the changes of binding potencies may not be directly related to the changes of side chain rotamer populations at position 8 because the backbone structural change around residues 8 and 9 may also be a contributing factor. However, a comparison was made between these two analogs (VII and VIII) and a cyclic hexapeptide (c[Pro-Phe-L-Trp-Lys-Thr-Phe]) which shows similar backbone conformations.[34] The (2S,3R)-β-MeTrp[8] side chain displayed a preference for the trans rotamer, while the (2S,3S)-β-MeTrp[8] side chain displayed a preference for the g^- rotamer, as indicated by the different chemical shifts of Lys[9] C^γ protons in analogs VII and VIII. The (2S,3R)-β-MeTrp[8] analog VII showed a 3-fold increase in binding potency when compared with c[Pro-Phe-L-Trp-Lys-Thr-Phe] (binding potency = 30 nM), while the (2S,3S)-β-MeTrp[8] analog VIII does not bind. These results are in agreement with the proposal that the trans rotamer is the "bioactive rotamer" for the side chain at position 8.

Unlike the Phe side chain, the χ_2 of the Trp[8] side chain is also an important parameter for conformation–activity relationships, as revealed in a previous study by Veber, Nutt, and co-workers.[14] Therefore, we examined the conformation around the χ_2 torsion in the β-MeTrp[8] side chain. Since no proton–proton coupling constant could be obtained for the χ_2 torsion, only NOE data were used to analyze the conformation around this torsion. Examinations of the NOEs for the β-MeTrp[8] C^βH and β-methyl group to the indole ring protons suggest different χ_2 torsions for the L-β-MeTrp[8] side chains and the D-β-MeTrp[8] side chains, which is in agreement with Veber's model.[14] On the other hand, the (2R,3S)- and (2R,3R)-β-MeTrp[8] side chains assume similar χ_2, and so do the (2S,3R)- and (2S,3S)-β-MeTrp[8] side chains. This may suggest that β-methyl chiral substitutions of either the D-Trp[8] or L-Trp[8] have a less significant effect on the χ_2 torsion than they do on the χ_1 torsion.

"Bioactive Conformation" of the Phe[11] Side Chain. The (2R,3S)- (XI) and (2R,3R)-β-MePhe[11] (XII) analogs display a trans amide bond at the bridging region, which leads to the loss of their binding affinities because the cis amide bond is required for bioactivity.[8] The (2S,3S)- (IX) and (2S,3R)-β-MePhe[11] (X) analogs maintain similar backbone conformations of the parent compound I, while their β-MePhe[11] side chains show different preferred conformations over the g^- and trans rotamers. As shown in Table VI, the (2S,3S)-β-MePhe[11] side chain displays a 26% increase in the g^- rotamer population, while the (2S,3R)-β-MePhe[11] side chain displays a 21% increase in the trans rotamer population when compared with the parent compound I. Differences in chemical shifts observed for these two analogs also support the different conformational preferences for the β-MePhe[11] side chains. These results, together with the evidence obtained for the β-MePhe[7] and β-MeTrp[8] side chains, consistently suggest that the side chain of the β-methylated residue is constrained to prefer the g^- rotamer for the 2S,3S isomer, the trans rotamer for the 2S,3R and 2R,3S isomers, and the g^+ rotamer for the 2R,3R isomer.

The (2S,3S)-β-MePhe[11] analog IX displayed an increased population over the g^- rotamer for the β-MePhe[11] side chain, while its binding potency decreased 50-fold when compared with the parent compound I. This suggests that the g^- rotamer is not the "bioactive rotamer" for the side chain at position 11. Meanwhile, the (2S,3R)-β-MePhe[11] analog X offered no direct evidence on the "bioactive conformation" for the β-MePhe[11] side chain since it did not bind to the somatostatin receptor. However, examination of other active analogs gives indication of the "bioactive conformation" of the Phe[11] side chain. As shown in Table VI, the active (2S,3R)-β-MeTrp[8] analog VII displayed a predominant trans rotamer for the Phe[11] side chain. This suggests that the trans rotamer is the "bioactive rotamer" for the Phe[11] side chain. To investigate the "bioactive conformation" of the Phe[11] side chain, Veber, Nutt, and co-workers synthesized cyclic hexapeptides c[N-MeAla[6]-Phe[7]-D-Trp[8]-Lys[9]-Thr[10]-Phe[11]] and c[N-MePhe[6]-

(34) NMR studies of c[Pro[6]-Phe[7]-L-Trp[8]-Lys[9]-Thr[10]-Phe[11]] indicated a β I turn around Trp[8]-Lys[9]. As for the bridging region, a cis/trans isomerism was observed for the amide bond between Phe[11]-Pro[6] with a ratio of 83:17. Huang, Z., et al. Unpublished results.

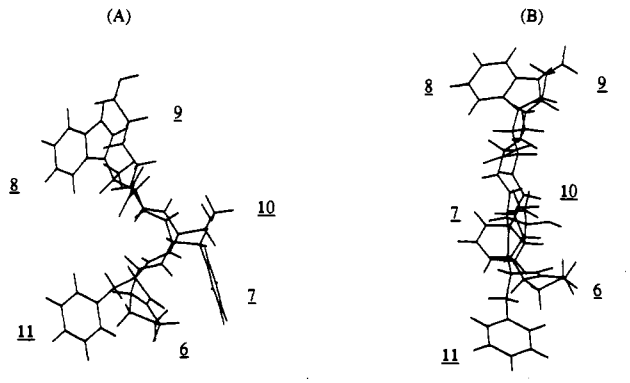

Figure 2. Possible conformations of the active c[Pro^6-Phe^7-(2*R*,3*S*)-β-MeTrp^8-Lys^9-Thr^{10}-Phe^{11}] (V). (A) "Folded" conformation and (B) "flat" conformation. The numbers refer to the locations of residues.

Phe^7-D-Trp^8-Lys^9-Thr^{10}-Ala^{11}] which contain the aromatic group at different locations of the bridging region.[16] They suggested that the trans conformation of the Phe^{11} side chain is important for bioactivity. In a collaborative study with Veber, we analyzed a series of active cyclic hexapeptide analogs synthesized by Veber and co-workers. These analogs contained changes in the location and the number of aromatic side chains at the bridging region.[35] Comparisons of the preferred side chain arrangements at the bridging region in these analogs also provided consistent evidence for the trans rotamer of the Phe^{11} side chain as the "bioactive conformation".

Overall Topochemical Array for Receptor Binding. Conformational searches have been carried out for the parent compound and the analogs containing side chain variations in order to find the accessible conformations consistent with NMR data. The comparison of accessible conformational space possessed by active and inactive analogs may enable us to define possible "bioactive conformations". Table VIII gives a summary of the possible conformations found for these analogs. All bioactive analogs can adopt two possible conformations which we define as "folded" and "flat" topologies, respectively, referring to their overall topochemical array of side chains and main chain. In both the "folded" and the "flat" conformations (Figure 2), the side chain of Trp^8 assumes the trans rotamer while the side chain of Lys^9 assumes the g^- rotamer, thus allowing a close proximity between them. The Phe^{11} side chain assumes the trans rotamer. The peptide backbone adopts a β II′ turn about residues 8 and 9 and a β VI turn with a cis amide bond about residues 6 and 11. The key difference between the "folded" and "flat" conformers is the different backbone torsions for residues 7 and 10. The "flat" conformer shows a C_5 or planar β sheet conformation for residues 7 and 10, while in the "folded" conformer, the overall topology is folded around residues 7 and 10, assuming a C_7 conformation. Dramatic changes are observed for the distances between the side chain of Phe^{11} and the side chains of Trp^8 and Lys^9 in these two conformations. In the "flat" conformation, the side chains of Trp^8 and Lys^9 display large separation (about 12 Å) from the side chain of Phe^{11}, while much smaller distances of about 8 and 9 Å, respectively, are observed in the "folded" conformation. Both the "folded" and "flat" conformations are consistent with all NMR data. Energy calculations using low dielectric constants indicate that the "folded" conformation is lower in energy than the "flat" conformation. At high dielectric constants, energies for these two conformations are almost equal. The "folded" conformation is believed to be favored at low dielectric constants, because more internal hydrogen bonds are present in the "folded" conformation than in the "flat" conformation. The "folded" and "flat" conformations found in this study are in agreement with the "cup" shaped and "flat" structures reported by Veber.[36] It should be pointed out that the (2*S*,3*R*)-β-MeTrp^8 analog **VII** contains an L-Trp^8 residue instead of a D-Trp^8 residue, as seen in other active analogs. Even though this L-Trp^8-containing analog **VII** adopts a β I turn about Trp^8-Lys^9 instead of the β II′ turn in the D-Trp^8-containing analogs, its overall topology is very similar to that of D-Trp^8-containing analogs, which is indicated by a similar set of side chain–side chain distances, as shown in Table VIII. These results suggest that overall topology is not sensitive to the structural changes around Trp^8-Lys^9 region.

To investigate whether the "folded" or "flat" conformation is the "bioactive conformation", we have extended the approach of side chain chiral methylations to the main chain and synthesized two diastereomers (**XIII** and **XIV**) containing α-MePhe at position 7. Our design of the α-MePhe^7 analogs is based on the results from energy minimization studies which indicated that, because of the steric effect introduced by the α-methyl group, the α-MePhe^7 backbone is constrained to prefer the C_5 conformation, and therefore the "flat" conformation is favored while the "folded" conformation is not allowed. This allowed us to examine the recent proposal by Veber stating that the "flat" conformation is the "bioactive conformation".[36] Since the (*R*)-α-MePhe^7 analog **XIV** has a D-configuration for residue 7 and displays conformations different from either the "folded" or "flat" conformation, we focused our analyses on the (*S*)-α-MePhe^7 analog **XIII**. The NOEs of Trp^8 C$^\alpha$H–Lys^9 NH and Lys^9 NH–Thr^{10} NH and the coupling constants of Trp^8 and Lys^9 suggest a β II′ turn about D-Trp^8-Lys^9 region. The low temperature coefficient measured for the Thr^{10} amide (about 0.30 ppb/K) is consistent with a hydrogen bond between Thr^{10} NH and α-MePhe^7 CO which stabilizes the β II′ turn. As for the bridging region, the strong NOE between Phe^{11} C$^\alpha$H and Pro^6 C$^\alpha$H indicates a cis amide bond. These results suggest that the (*S*)-α-MePhe^7 analog **XIII** maintains similar conformations about the D-Trp^8-Lys^9 region and the bridging region of the parent compound **I**. The mutual strong NOEs of Trp^8 NH, the α-methyl group, and α-MePhe^7 C$^\beta$H confirm the C_5 conformation for the α-MePhe^7 backbone, because only in the C_5 conformation can these protons display such spatial relationships. In the C_7 conformation, only the strong NOE of Trp^8 NH and α-methyl group would be expected. As a result, the α-MePhe^7 analog **XIII** displays a "flat" conformation. Both analogs **XIII** and **XIV** have been tested and display very low binding affinities (Table I). These results are inconsistent with the "flat" model as proposed by Veber. Therefore, we suggest that the "folded" conformation is likely to be the "bioactive conformation". The superposition of all active molecules in the "folded" conformation defines important topochemical arrays necessary for binding to a somatostatin receptor. As revealed in this superposition, the Phe^7 side chain may provide a less strict conformational region because a large space is allowed for this side chain. On the other hand, the side chains of Trp^8 and Lys^9, a folded peptide backbone, and the side chain of Phe^{11} form a binding "pocket" essential for a peptide approaching a receptor. Our model provides a consistent explanation for the active analogs. Furthermore, we applied this model to examine the possible causes of loss of binding affinities for inactive analogs.

Chiral Effect of the β-Methyl Group on Receptor Binding. Analogs **VI**, **VIII**, and **X**–**XII** are inactive in the binding assay, which suggests that either these molecules cannot adopt the active topochemical array as described above or there are steric interactions which prohibit receptor binding if these molecules do adopt a "bioactive conformation". As we have already discussed, the (2*R*,3*S*)- (**XI**) and (2*R*,3*R*)-β-MePhe^{11} (**XII**) analogs show a trans amide bond at the bridging region which lead to the loss of their binding affinities. However, for the (2*R*,3*R*)-β-MeTrp^8 analog **VI**, (2*S*,3*S*)-β-MeTrp^8 analog **VIII**, and the (2*S*,3*R*)-β-MePhe^{11} analog **X**, the loss of binding affinities cannot be accounted for by backbone conformations, because results from conformational searches indicate that these analogs can adopt backbone structures

(35) NMR studies were carried out for c[N-MeAla-Tyr-D-Trp-Lys-Val-Phe], c[N-MeAla-Phe-L-Trp-Lys-Thr-Phe], c[N-MePhe-Phe-D-Trp-Lys-Thr-Ala], and c[N-MePhe-Phe-D-Trp-Lys-Thr-Phe]. Huang, Z., et al. Unpublished results.

(36) Veber, D. F. In *Peptides: Chemistry and Biology, Proceedings of the Twelfth American Peptide Symposium*; Smith, J. A., Rivier, J. E., Eds.; ESCOM: Leiden, 1992; pp 3–14.

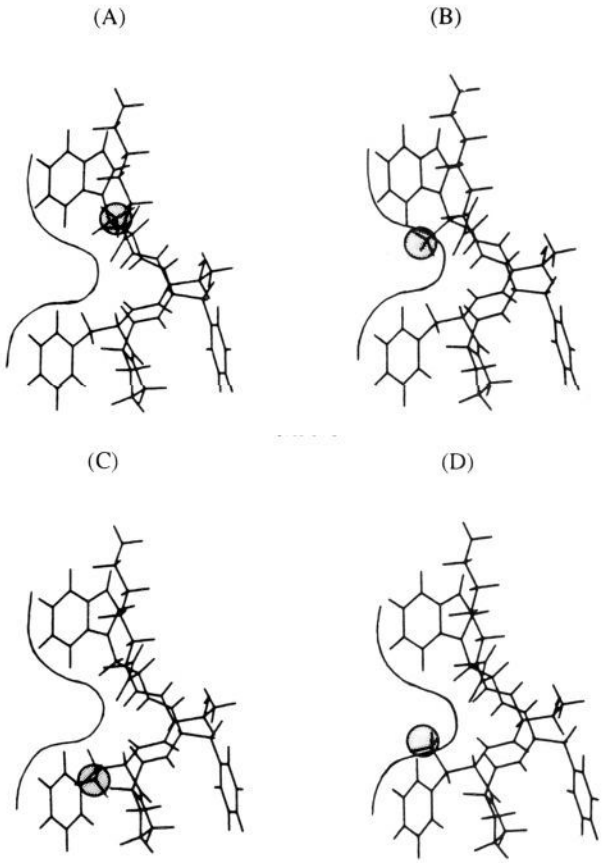

Figure 3. Comparison of the projections of β-methyl groups of (A) active (2*R*,3*S*)-β-MeTrp[8] analog **V**, (B) inactive (2*R*,3*R*)-β-MeTrp[8] analog **VI**, (C) active (2*S*,3*S*)-β-MePhe[11] analog **IX**, and (D) inactive (2*S*,3*R*)-β-MePhe[11] analog **X**. The methyl groups are highlighted by shaded spheres.

similar to those found for active analogs. Even though the modified side chain is constrained into a rotamer different from the active form due to the β-methyl substitution, we may not be able to exclude the possibility of these inactive analogs adopting a "bioactive conformation". In other words, the changes of side chain rotamer population seen in the inactive analogs can contribute to the diminished binding potency, but this is not enough to explain the total loss of binding. Therefore, we suggest that the β-methyl substitution has a chiral effect by which the different projections of a β-methyl group, in certain cases, invokes steric hindrance to receptor binding. Figure 3 shows the comparison of two pairs of active and inactive diastereomers in the proposed "bioactive conformation". It can be seen that in the (2*R*,3*R*)-β-MeTrp[8]- (**VI**) and (2*S*,3*R*)-β-MePhe[11] (**X**) analogs, the β-methyl group is projected into the proposed binding "pocket". We suggest that the steric hindrance created by a methyl group in this "pocket" prevents these two analogs from binding to a somatostatin receptor, even when the molecules assume the "bioactive conformation".

As for the (2*S*,3*S*)-β-MeTrp[8] analog **VIII**, it seems that the projection of the β-methyl group does not have any steric effect on receptor binding. However, a closer examination indicates that the β-methyl group projects into the space between side chains of Trp[8] and Lys[9], thus creating unfavorable steric interactions which cause the side chains of Trp[8] and Lys[9] to move away from each other and therefore destabilize the "bioactive conformation". To examine our hypothesis, we have carried out 100-ps molecular dynamics simulations for the analog **VIII**, the active (2*S*,3*R*)-β-MeTrp[8] analog **VII**, and the parent compound **I**. Dynamics simulations for these three analogs were started with a similar "bioactive conformation". Because of the steric effect caused by the β-methyl group, the inactive (2*S*,3*S*)-β-MeTrp[8] analog **VIII** underwent a conformational change shortly after the start of dynamics simulations in which the Trp[8] and Lys[9] side chains

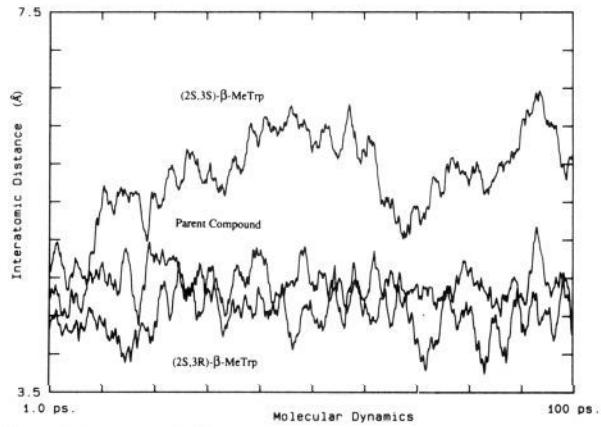

Figure 4. Interatomic distance during a 100-ps timecourse of molecular dynamics for the Cγ atoms of the Trp[8] and Lys[9] side chains of the three somatostatin analogs (**I**, **VII**, and **VIII**).

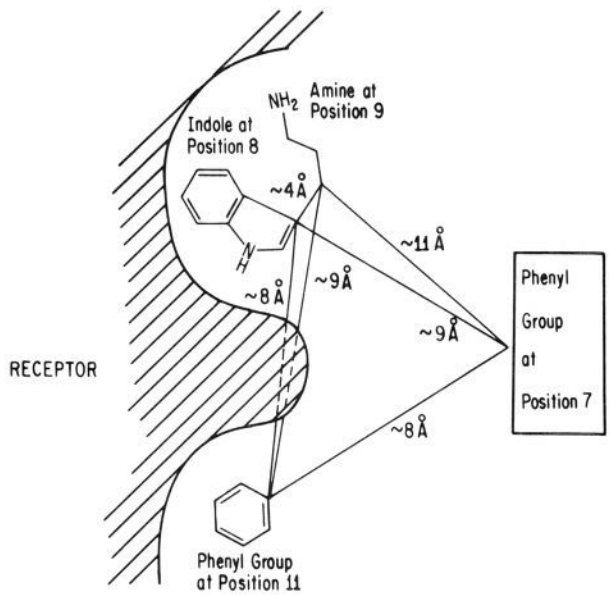

Figure 5. Schematic model for somatostatin pharmacophores.

moved away from each other. The (2*S*,3*R*)-β-MeTrp[8] analog **VII** remained essentially in the "bioactive conformation" with the side chains of Trp[8] and Lys[9] in close proximity throughout the dynamics. Figure 4 shows the comparison of the distances between the Trp[8] and Lys[9] side chains during molecular dynamics for the (2*S*,3*S*)- (**VIII**) and (2*S*,3*R*)-β-MeTrp[8] (**VII**) analogs and the parent compound **I**. The side chains of Trp[8] and Lys[9] in the active (2*S*,3*R*) analog **VII** displayed close interactions similar to those of the parent compound **I**, while a large separation was observed for the inactive (2*S*,3*S*) analog **VIII**. These results support our contention that, in the (2*S*,3*S*)-β-MeTrp[8] analog **VIII**, the β-methyl group sterically hinders the close proximity of the Trp[8] and Lys[9] side chains, which is necessary for binding.

To summarize our findings from these α-methylated and β-methylated somatostatin analogs, we propose a schematic model to illustrate the important topochemical requirements for binding to a somatostatin receptor. As shown in Figure 5, the side chains of Trp[8], Lys[9], and Phe[11] in the displayed topological array constitute the most essential elements necessary for binding. We suggest that, using this model, novel somatostatin agonists with peptide or nonpeptide backbone templates can be designed.

Conclusions

We have developed an integrated approach for investigating main chain and side chain conformations important for the binding of somatostatin analogs. The "bioactive conformations" for the

side chains of Phe[7], Trp[8], and Phe[11] in the parent cyclic hexapeptide I have been derived from the analyses of the conformational and biological effects of β-methyl substitutions at these residues. Definitive evidence has been obtained about the "bioactive conformations" of Trp[8] and Phe[11] side chains as proposed by Veber.[8] As pointed out by Veber,[8] we found a close interaction between the side chains of Trp[8] and Lys[9] for active analogs. We have also gained new insights into the conformational space for the Phe[7] side chain when bound to a receptor. As for the backbone structure, we confirm the β II′ turn around Trp[8]-Lys[9] and the β VI turn around Phe[11]-Pro[6] with a cis amide bond, as proposed by Veber.[8] Analyses of the α-methylated analogs suggest a C_7 conformation for the Phe[7] and Thr[10] backbone, which folds the peptide into a topochemical array important for receptor binding. Finally, we propose a binding "pocket" consisting of the side chains of Trp[8], Lys[9], and Phe[11] supported by a folded backbone, which should be an important consideration in the future design of somatostatin analogs.

It is important to find that the β-methyl substitution has two profound effects on the structure and bioactivity of somatostatin analogs. First, it specifically constrains the flexible side chains to prefer particular rotamers depending on the chiralities of the C^β atom while maintaining the backbone conformation of the parent cyclic hexapeptide. For instance, the side chain of Trp[8] in the parent compound I shows a large degree of flexibility, with almost equal populations over the trans and g^+ rotamers. Upon β-methyl substitution, this side chain adopts predominantly, but not exclusively, the trans and g^+ rotamers for the 2*R*,3*S* (V) and 2*R*,3*R* (VI) diastereomers, respectively. The 2*R*,3*S* analog V is more potent than the parent compound I, while the 2*R*,3*R* analog VI is less potent by more than 1000-fold. The structure of the modified side chain and the resulting enhanced binding potency provide evidence for specific topochemical arrays of the side chains required for interaction with the receptor. Second, the projection of the chiral β-methyl group into specific conformational space affects interactions with the receptor. This provides a powerful means of probing the topochemical nature of the binding site. As in the cases of (2*R*,3*S*)- (V) and (2*R*,3*R*)-β-MeTrp[8] (VI) and (2*S*,3*S*)- (IX) and (2*S*,3*R*)-β-MePhe[11] (X) analogs, the comparison of the spatial projections of the β-methyl groups in these analogs reveals crucial insight into a binding "pocket" required for a peptide interacting with a receptor.

Finally, many peptide hormones and neurotransmitters have key aromatic side chains important for their receptor binding and transduction mechanisms. The chiral methylation approach we use in this study of somatostatin analogs should have important implications on the design and analysis of other peptide ligands, such as opioids, taste ligands, oxytocins, LHRH, CCK antagonists, etc.

Experimental Section

General Data. Melting points, determined on a Thomas Hoover capillary melting point apparatus, were uncorrected. Nuclear magnetic resonance spectroscopy of the intermediates was carried out on a General Electric QE-300 spectrometer. Microanalyses were provided by Desert Analytics, Tucson, AZ. Fast-atom bombardment mass spectra were obtained from the University of California, Riverside. Amino acid analysis was performed at Scripps Research Institute, La Jolla. High-pressure liquid chromatography was run on a Waters HPLC system, equipped with two 510 solvent pumps, a Waters 484 detector, and a Perkin-Elmer LC1-100 integrator. Thin layer chromatography was carried out on precoated silica gel 60 (F_{254}) plates using the following solvent system: (A) $CHCl_3$:MeOH:AcOH 22:1:1; (B) $CHCl_3$:MeOH:NH_4OH 85:32:5. The compounds were visualized by UV light, chlorine/*o*-tolidine, ninhydrin, and vanillin.

Boc-(2*R*,3*S* + 2*S*,3*R*)-β-MeTrp-OH (4a). A solution of BocON (4.74 g, 19.26 mmol) in dioxane (12 mL) was added to the mixture of threo isomers of H-β-MeTrp-OH (**3a**) (2.80 g, 12.84 mmol) and Et_3N (2.7 mL, 19.26 mmol) in H_2O (12 mL) under nitrogen at room temperature. The reaction was complete in 5 h. The reaction mixture was concentrated under reduced pressure, and the residue was acidified to pH 3.5–4 with an aqueous solution of sodium bisulfate, extracted with ethyl acetate (4 × 60 mL), dried over $MgSO_4$, and concentrated. Recrystallization from ethyl acetate/hexane yielded 2.83 g (69%) of **4a** as a white solid: mp 159.5–161 °C; ^{1}H NMR (DMSO-d_6) δ 12.39 (br, 1 H, COOH), 10.83 (s, 1 H, indole-NH), 7.52–6.94 (m, 5 H, indole), 6.94 (d, *J* = 8.4 Hz, 1 H, NH), 4.26 (dd, *J* = 8.4, 6.5 Hz, 1 H, C^αH), 3.52 (dt, *J* = 6.5, 7.2 Hz, 1 H, C^βH), 1.34 (s, 9 H, Boc), 1.30 (d, *J* = 7.2 Hz, 3 H, Me); MS *m*/*z* 318 (M^+). Anal. Calcd for $C_{17}H_{22}N_2O_4$: C, 64.13; H, 6.97; N, 8.80. Found: C, 64.01; H, 6.79; N, 8.58.

Boc-(2*R*,3*R* + 2*S*,3*S*)-β-MeTrp-OH (4b): yield 73%; mp 177.5–179 °C; ^{1}H NMR (DMSO-d_6) δ 12.52 (br 1 H, COOH), 10.85 (s, 1 H, indole-NH), 7.55–6.95 (m, 5 H, indole), 6.36 (d, *J* = 8.1 Hz, 1 H, NH), 4.25 (dd, *J* = 8.1, 6.6 Hz, 1 H, C^αH), 3.45 (dt, *J* = 6.6, 6.8 Hz, 1 H, C^βH), 1.32 (s, 9 H, Boc), 1.28 (d, *J* = 6.8 Hz, 3 H, Me); MS *m*/*z* 318 (M^+). Anal. Calcd for $C_{17}H_{22}N_2O_4$: C, 64.13; H, 6.97; N, 8.80. Found: C, 64.01; H, 6.92; N, 8.70.

Boc-Pro-(*SR*)-α-MePhe-OMe (6). A methanol solution (35 mL) of a racemic mixture of H-α-MePhe-OH (**5**) (4.8 g, 26.82 mmol) and thionyl chloride (4 mL) was refluxed for 20 h. After the solvent was removed, the crude product HCl·H-α-MePhe-OMe (4.7 g) was dissolved in DMF (120 mL), and the solution was cooled to −40 °C. The mixture was neutralized by DIEA followed by addition of Boc-Pro-OH (6.28 g, 29.21 mmol), HOBt (3.94 g, 29.19 mmol), and EDC·HCl (7.01 g, 36.53 mmol) consecutively. The reaction mixture was warmed to room temperature and stirred overnight, followed by concentration under reduced pressure. The residue was diluted with ethyl acetate (300 mL), washed with an aqueous solution of $NaHCO_3$ and brine, dried over $MgSO_4$, and concentrated. Column chromatography on silica gel (hexane/ethyl acetate 10/2) gave 5.64 g (54%) of **6** as an oily material: ^{1}H NMR (DMSO-d_6) δ 8.07 & 8.00–7.90 (s, m, 1 H, NH), 7.35–7.05 (m, 5 H, Ph), 4.17–4.07 (m, 1 H, C^αH), 3.55 (s, 3 H, OCH_3), 3.40–3.20 (m, 2 H, Pro), 3.17–2.90 (m, 2 H, C^βH, α-MePhe), 2.15–1.95 (m, 1 H, Pro), 1.87–1.68 (m, 3 H, Pro), 1.37 (s, 3 H, CH_3), 1.34 (s, 9 H, Boc); MS *m*/*z* 391 (M + H)$^+$. Anal. Calcd for $C_{21}H_{30}N_2O_5$: C, 64.59; H, 7.74; N, 7.17. Found: C, 64.29; H, 7.67; N, 7.18.

Boc-Pro-(*SR*)-α-MePhe-OH (7). A mixture of **6** (5.62 g, 14.41 mmol) and LiOH (630 mg, 15 mmol) in H_2O (30 mL) and THF (100 mL) was stirred at room temperature for 12 h, and then a second portion of LiOH (315 mg, 7.5 mmol) was added. The reaction mixture was stirred for 36 h, followed by concentration under reduced pressure at room temperature. The residue was acidified to pH 3.5–4 with an aqueous solution of sodium bisulfate, extracted with ethyl acetate (3 × 150 mL), dried over $MgSO_4$, and concentrated. Column chromatography on silica gel (hexane/ethyl acetate 5/5 followed by ethyl acetate) gave 4.50 g (83%) of **7** as a white solid: mp 66–67.5 °C; ^{1}H NMR (DMSO-d_6) δ 12.65 (br, 1 H, COOH), 7.90–7.50 (m, 1 H, NH), 7.40–7.00 (m, 5 H, Ph), 4.20–4.00 (m, 1 H, C^αH), 3.45–3.00 (m, 4 H, Pro, C^βH Phe), 2.10–1.65 (m, 4 H, Pro), 1.34 (br, 12 H, Boc, CH_3); MS *m*/*z* 377 (M + H)$^+$. Anal. Calcd for $C_{20}H_{28}N_2O_5$: C, 63.81; H, 7.50; N, 7.44. Found: C, 63.90; H, 7.39; N, 7.35.

Syntheses of Cyclic Hexapeptides II–IV and IX–XIV, General Method.[37] **c[Pro-(2*S*,3*R*)-β-MePhe-D-Trp-Lys-Thr-Phe] (III).** Peptide synthesis was carried out on a manually operated solid-phase synthesis apparatus using *p*-nitrobenzophenone oxime resin prepared according to the literature.[38] Boc-Thr(OBzl)-OH (772 mg, 2.50 mmol) was attached to the oxime resin (4.50 g) with DCC (515 mg, 2.50 mmol) in DCM (70 mL) at room temperature overnight, followed by acylation with a mixture of pivalic anhydride (6.75 mL) and DIEA (2.25 mL) in DCM (60 mL) for 3 h, yielding 4.90 g (substitution level 0.26 mmol/g resin based on picric acid titration,[39] 1.27 mmol of amino acid). The obtained Boc-Thr(OBzl)-resin was deprotected with 25% TFA/DCM (30 min) and neutralized with 5% DIEA/DCM. A DCM solution of symmetrical anhydride of Boc-Lys(2Cl-Z)-OH[24] (3.81 mmol) was poured into the reaction vessel. After the reaction mixture was shaken for 1 h, a Kaiser test indicated that the coupling reaction was complete. Boc-D-Trp-(For)-OH was treated in the same manner to give Boc-Trp(For)-Lys-(2Cl-Z)-Thr(OBzl)-resin (5.54 g, substitution level 0.207 mmol/g resin based on picric acid titration,[39] 1.15 mmol of peptide). The peptide chain elongation was continued by using Boc-Trp(For)-Lys(2Cl-Z)-Thr-(OBzl)-resin (800 mg, 0.166 mmol of peptide) for consecutive addition of the following amino acids: Boc-(2*S*,3*R*)-β-MePhe-OH, Boc-Pro-OH, and Boc-Phe-OH. The product, Boc-Phe-Pro-(2*S*,3*R*)-β-MePhe-D-Trp-(For)-Lys(2Cl-Z)-Thr(OBzl)-resin was obtained. After the Boc group was cleaved, the cyclization reaction was carried out on the resin in DCM (15 mL) and DMF (15 mL) in the presence of 10 equiv of AcOH at room temperature for 72 h. The crude cyclic peptide (140 mg) was obtained after filtration and evaporation. Amino acid analysis: Lys 1.00, Thr 0.91, Phe 1.12, Pro 1.10. R_f(A): 0.58. FABMS *m*/*z* 1108 (M +

(37) All the washing steps were omitted.

(38) (a) DeGrado, W. F.; Kaiser, E. T. *J. Org. Chem.* **1980**, *45*, 1295–1300. (b) DeGrado, W. F.; Kaiser, E. T. *J. Org. Chem.* **1982**, *47*, 3258–3261.

(39) Gisin, B. F. *Anal. Chim. Acta* **1972**, *58*, 248–249.

H)$^+$. The peptide was treated with HF/anisole/skatole (20 mL/0.5 mL/3 mg) at −10 °C for 30 min and at 0 °C for 30 min to give an oily material (85 mg), which was treated with piperidine (25 mL) 3 h at room temperature. Purification of the final product III was carried out on RP-HPLC to yield 31 mg (18% based on Boc-Thr(OBzl)-resin). Physical properties and analytical data for the peptides II–IV and IX–XIV are summarized in Table II.

Syntheses of Cyclic Hexapeptides V–VIII, General Method.[37] **c[Pro-Phe-(2*R*,3*S*)-β-MeTrp-Lys-Thr-Phe] (V) and c[Pro-Phe-(2*S*,3*R*)-β-MeTrp-Lys-Thr-Phe] (VII).** Boc-Thr(OBzl)-Merrifield resin (915 mg, substitution level 0.73 mmol/g resin, 0.668 mmol of amino acid) purchased from Bachem was deprotected with TFA/anisole/DCM (50/2/48) (30 min) and neutralized with 5% DIEA/DCM. A DMF solution of Boc-Lys(Fmoc)-OH (904 mg, 2.00 mmol), BOP (884 mg, 2.00 mmol), and DIEA (775 mg, 6.01 mmol) was poured into the reaction mixture. The coupling reaction was complete in 2 h, as indicated by a Kaiser test. The peptide chain was then assembled by consecutive deprotection of Boc groups and addition of Boc-(2*R*,3*S* + 2*S*,3*R*)-β-MeTrp-OH, Boc-Phe-OH, Boc-Pro-OH, and Boc-Phe-OH as above. Thus, Boc-Phe-Pro-Phe-(2*R*,3*S* + 2*S*,3*R*)-β-MeTrp-Lys(Fmoc)-Thr(OBzl)-resin (1.42 g) was obtained. Amino acid analysis: Phe 2.00, Thr 1.00, Lys 0.87, Pro 1.04. The above peptidyl resin was treated with HF/anisole/skatole (24 mL/1.4 mL/10 mg) at −10 °C for 30 min and 0 °C for 30 min. The resulting peptide was dissolved in AcOH (80%, 15 mL), and the resin was removed by filtration. Separation and purification of the two diastereomers were carried out on RP-HPLC (Water C_4 proteins preparative cartridge; eluent 45% CH_3CN/H_2O with 0.1% TFA; flow rate 8 mL/min; detection at 215 nm). H-Phe-Pro-Phe-(2*R*,3*S*)-β-MeTrp-Lys-(Fmoc)-Thr-OH·TFA, yield: 282 mg (72% based on the starting Boc-Thr(OBzl)-resin); t_R 35.1 min; R_f(B) 0.56; HR-FABMS calcd for $C_{60}H_{69}N_8O_{10}(M + H)^+$ m/z 1061.5137, found 1061.5092. Amino acid analysis: Phe 2.00, Lys 0.75, Thr 1.13, Pro 1.02. H-Phe-Pro-Phe-(2*S*,3*R*)-β-MeTrp-Lys(Fmoc)-Thr-OH·TFA, yield: 215 mg (54% based on the starting Boc-Thr(OBzl)-resin); t_R 24.5 min; R_f(B) 0.49; HR-FABMS calcd for $C_{60}H_{69}N_8O_{10}(M + H)^+$ m/z 1061.5137, found 1061.5168. Amino acid analysis: Phe 2.00, Lys 0.85, Thr 1.03, Pro 0.94.

The compound H-Phe-Pro-Phe-(2*R*,3*S*)-β-MeTrp-Lys(Fmoc)-Thr-OH·TFA (61 mg, 0.052 mmol) was dissolved in DMF (54 mL). DPPA (17 mg, 0.062 mmol)-DMF (1 mL) and K_2HPO_4 (49 mg, 0.282 mmol) were added under nitrogen at 0 °C. The coupling reaction was carried out at 4 °C for 84 h. Bio-Red (AG 501-X8(D)) (2.0 g) was then added, and the mixture was stirred at 4 °C for 2.5 h. After filtration, the solution was evaporated under reduced pressure, and the residue was treated with piperidine (10 mL) for 4 h at room temperature. Purification of the final product V was carried out by RP-HPLC to yield 12.8 mg (19% based on Boc-Thr(OBzl)-resin). c[Pro-Phe-(2*S*,3*R*)-β-MeTrp-Lys-Thr-Phe] (VII) was obtained by the same cyclization method from H-Phe-Pro-Phe-(2*S*,3*R*)-β-MeTrp-Lys(Fmoc)-Thr-OH·TFA to yield 11 mg (11% based on Boc-Thr(OBzl)-resin). Physical properties and analytical data for the peptides V–VIII are summarized in Table II.

Binding Procedures. The binding of different peptides to the somatostatin receptor was performed as previously described.[40] Briefly, AtT-20 cells, which express a high density of somatostatin receptor, were detached from the culture flasks in which they were growing in phosphate buffered saline, the cells were homogenized with a Brinkman polytron (setting 1, 15 s), and the membranes were centrifuged at 20000*g* for 15 min at 4 °C. The pellet was resuspended, and the membranes were incubated in a buffer containing 50 mM Tris-HCl (pH 7.4), 1 mM EDTA, 5 mM $MgCl_2$, 10 μg/mL of leupeptin, 10 μg/mL of pepstatin, 200 μg/mL of bacitracin, and 0.5 μg/mL of aprotinin with 0.05 nM ^{125}I-MK 678 (specific activity 2000 Ci/mmol) in the presence or absence of various somatostatin analogs for 60 min at 25 °C. The reaction was terminated by adding 15 mL of ice-cold Tris-HCl (pH 7.8) buffer and vacuum filtering under reduced pressure over Whatman GF/C glass fiber filters. Radioactivity was assessed in a gamma counter (80% efficiency). Nonspecific binding was determined by the residual radioligand binding remaining in the presence of 1 μM somatostatin, and specific binding accounted for 80–85% of total ^{125}I-MK 678 binding. The potency of each peptide for the somatostatin receptor was assessed by determining the ability of different concentrations of the peptide to inhibit ^{125}I-MK 678 binding and then analyzing the inhibition curve using the PROPHET data analysis system. Affinities are expressed as IC_{50} values, and each IC_{50} is the averaged results of three different experiments for each peptide.

NMR Measurements. The ^{1}H NMR spectra were recorded on either a General Electric GN-500 or a Bruker AMX spectrometer operating at 500 MHz. Temperatures were maintained at given values within ±0.1 °C during measurements. The samples were prepared in DMSO-d_6 purchased from Merck Sharp and Dohme Canada Ltd. at a concentration of 5–15 mM. DMSO-d_6 (=2.49 ppm) was used as an internal standard.

The one-dimensional spectra contain 16K data points in 6000–7000 Hz. The two-dimensional homonuclear Hartmann–Hahn (HOHAHA) experiments[41] were carried out using the MLEV17[42] and the time-proportional phase increment.[43] A mixing time of 100 ms (48 cycles of MLEV sequence) with a spin locking field of 10.2 kHz was employed. The rotating frame nuclear Overhauser (ROESY) experiments[44] were carried out varying the mixing time from 75 ms to 500 ms with a spin locking field of 2.5 kHz. All of the two-dimensional spectra were obtained using 2K data points in the f_2 domain and 256 points in the f_1 domain. Applying the zero filling procedure to the f_1 domain twice resulted in a final matrix of 2K × 2K data points. Multiplication with either a phase shifted sine or a Gaussian function was used to enhance the spectra.

Computer Simulations. All calculations were performed on a Personal Iris 4D-25 workstation and an Iris 4D-340 computer (Silicon Graphics). Energy minimizations and molecular dynamics computations were carried out with the molecular modeling package which included QUANTA 3.0 (Molecular Biosystems Inc.) and CHARMM.[45]

All hydrogen atoms were included in all calculations. The potential energy of the molecular system was expressed by the valence force field implemented in CHARMM (without an explicit hydrogen bonding term) with the PARM21A parameter set. A neutral form of the amine group in Lys side chain was used. To approximate the solvation, all calculations were carried out at a distance-dependent dielectric constant ($\epsilon = R$)[46] unless specified otherwise. Energy minimizations with respect to all the Cartesian coordinates were carried out using the Adopted Basis Newton-Raphson (ABNR) algorithm[45] until all derivatives were smaller than 0.001 kcal/mol Å.

Molecular dynamics simulations were undertaken by numerical integration of Newton's equations of motion with a second-order predictor two-step Verlet algorithm.[47] The SHAKE algorithm[48] was used, which allowed a step size of 1 fs in dynamics. All simulations were preceded by 1 ps of heating from 0 to 300 K, followed by a 2-ps equilibration period. Equilibrations and simulations were performed at 300 K. NOE constrains were not used in dynamics calculations.

Conformational searches were carried out to obtain low energy conformations consistent with NMR data. They included several steps. First, the distance geometry method[49] was applied to generate a set of 400 conformations using distance constraints derived from observed NOEs (the DGEOM program by Blaney and co-workers was obtained through QCPE, program #590). Ascribing a particular interproton distance to a strong, medium, or weak NOE is based on the assumption that the cross-peak intensity for a particular pair of protons depends only on the distance separating these protons. It has been shown that, even for relatively short mixing times, in multispin systems this approach systematically underestimates the distances.[50] With this in mind, we used ranges of 2.5 Å or less (but not less than the VDW lower limit) for strong, 2.5–3.0 Å for medium, and 3.0–4.0 Å for weak NOEs, which do not correspond to the simple inverse sixth power distance dependence. The structures so generated were then energy minimized without NOE constraints. Only minimized conformations within 10 kcal range above the lowest energy were further analyzed and divided into structural families on the basis of their backbone conformations. As a final step, starting with the lowest energy conformation of each structural families, χ_1 torsions of all side chains were varied systematically in 60° increments. The resulting new conformations were again minimized with respect to total potential energy. The final conformations were examined and selected according to their consistency with NOEs and a maximum de-

(40) Raynor, K.; Reisine, T. *J. Pharmacol. Exp. Ther.* **1989**, *251*, 510–517.

(41) Bax, A.; Davis, D. G. *J. Am. Chem. Soc.* **1985**, *107*, 2820–2821.

(42) (a) Bax, A.; Davis, D. G. *J. Magn. Reson.* **1985**, *65*, 355–360. (b) Levitt, M. H.; Freeman, R.; Frenkiel, T. *J. Magn. Reson.* **1982**, *47*, 328–330.

(43) Bodenhausen, G.; Vold, R. L.; Vold, R. R. *J. Magn. Reson.* **1980**, *37*, 93–106.

(44) Bothner-By, A. A.; Steppens, R. L.; Lee, J.; Warren, C. D.; Jeanloz, R. W. *J. Am. Chem. Soc.* **1984**, *106*, 811–813.

(45) (a) Brooks, B. R.; Bruccoleri, R. E.; Olafson, B. D.; States, D. J.; Swaminathan, S.; Karplus, M. *J. Comput. Chem.* **1983**, *4*, 187. (b) Nilson, L.; Karplus, M. *J. Comput. Chem.* **1986**, *7*, 591.

(46) McCammon, J. A.; Wolynes, P. G.; Karplus, M. *Biochemistry* **1979**, *18*, 927–942.

(47) Verlet, L. *Phys. Rev.* **1967**, *159*, 98–103.

(48) Van Gunsteren, W. F.; Berendsen, H. J. C. *Mol. Phys.* **1977**, *34*, 1311.

(49) Crippen, G. M.; Havel, T. F. In *Distance Geometry and Molecular Conformation*; Research Studies Press: New York, 1988.

(50) Borgias, B. A.; James, T. L. *J. Magn. Reson.* **1988**, *79*, 493–512.

viation less than 25° for any single ϕ torsion estimated from the $J_{NH-H\alpha}$ coupling constants.

Acknowledgment. We wish to thank the National Institute of Health (DK 15410) for their support of this research. We also thank Drs. Toshimasa Yamazaki, Yun-Fei Zhu, and George Ösapay for many helpful discussions.

Supplementary Material Available: Experimental descriptions for syntheses of **1a**, **1b**, **2a**, and **2b**, as well as physical properties and analytical data for several intermediate protected linear and cyclic hexapeptides; Supplemental Scheme 1 for preparation of **1a** and **1b**; Supplemental Scheme 2 for synthesis of the peptides **V-VIII**; X-ray structural data for threo N-acetyl β-MeTrp-OH; tables of chemical shifts, $J_{NH-H\alpha}$ vicinal coupling constants, and calculated ϕ torsions for analogs containing side chain variations at positions 7 and 11 (16 pages); observed and calculated structure factors for $C_{14}H_{16}N_2O_3$ (11 pages). Ordering information is given on any current masthead page.

Syntheses of Racemic and Both Chiral Forms of Cyclopropane-*1,2-d*$_2$ and Cyclopropane-*1*-^{13}*C-1,2,3-d*$_3$

John E. Baldwin* and Steven J. Cianciosi

Contribution from the Department of Chemistry, Syracuse University, Syracuse, New York 13244. *Received April 2, 1992*

Abstract: The racemic and both chiral forms of cyclopropane-*1,2-d*$_2$ and cyclopropane-*1*-^{13}*C-1,2,3-d*$_3$ have been prepared efficiently through sequences based on *trans*-1,2-bis(methoxycarbonyl)cyclopropanes. These diesters have been prepared in racemic form with 1,2-d_2 labeling and with 3-^{13}C-1,2,3-d_3 labeling. The labeled diesters have been resolved to provide both chiral forms, and the racemic or resolved diesters have been converted to the corresponding specifically labeled racemic or chiral cyclopropanes through a two-step sequence involving reduction and decarbonylation. The chemical, isotopic, geometrical, and chiral quality of the labeled cyclopropanes in both sets of isomers is estimated to be quite high and strictly comparable.

The geometrical isomerization of the cis and trans forms of cyclopropane-*1,2-d*$_2$ was discovered by Rabinovitch, Schlag, and Wiberg in 1958,[1] and the optical isomerization interconverting directly the two chiral trans-1,2-*d*$_2$ cyclopropanes was demonstrated by Berson and Pedersen in 1975.[2] These stereomutation reactions result from one-center or two-center epimerization processes and are thought to be mediated by singlet trimethylene diradical structures.[3]

Between 1975 and 1990 these reactions were not subject to further experimental study. Theoretical efforts to understand these stereomutations were sustained, and experimental investigations with cyclopropanes substituted with functional groups or with functional groups and deuterium labels were pursued.[3,4] But kinetic studies with isotopically substituted cyclopropanes, the systems most likely to provide a meaningful link between theory and experiment, were not conducted, in spite of the fact that the fundamental experimentally accessible characteristic of these reactions—the relative kinetic significance of one-center versus two-center epimerization events[5]—remained uncertain.

This hiatus in experimental activity may have been due to perceived synthetic limitations, for without efficient routes to selected isotopically labeled and chiral cyclopropanes, the information they could provide through kinetic studies remained unavailable. Or this hiatus may have been consequent to a conceptual limitation: just how one might gain experimental access to the k_1/k_{12} ratio by following the thermal stereomutations of a suitably selected isotopically labeled cyclopropane was not immediately obvious. Or, possibly, some might have imagined that the experimental problem had been solved.

This paper reports in full detail efficient preparations of racemic and both optically active forms of cyclopropane-*1,2-d*$_2$, **1**-*d*$_2$, (*rac*-**1**-*d*$_2$), (*S,S*)-**1**-*d*$_2$, and (*R,R*)-**1**-*d*$_2$, and of racemic and both optically active forms of cyclopropane-*1*-^{13}*C-1,2,3-d*$_3$, **1**-^{13}*C,d*$_3$, (2*R*,3*R*)-**1**-^{13}*C,d*$_3$, and (2*S*,3*S*)-**1**-^{13}*C,d*$_3$. The d_2 cyclopropanes

(*S,S*)-**1**-d_2 (*R,R*)-**1**-d_2

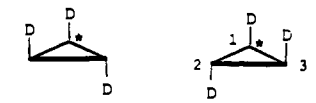

(2*R*,3*R*)-**1**-^{13}C,d_3 (2*S*,3*S*)-**1**-^{13}C,d_3

have been used to confirm[6] the experimental findings (the relative magnitures of rate constants for geometrical isomerization, k_i, and for racemization, k_a) reported in 1975 by Berson and Pedersen,[2] while the chiral cyclopropane-*1*-^{13}*C-1,2,3-d*$_3$ compounds have permitted access to an experimentally determined measure of one-center versus two-center epimerizations. These modes of thermal stereomutation are of comparable kinetic importance: for this isotopically labeled system at 407 °C, k_1/k_{12} is (0.95 ± 0.09)/1.[7]

The credibility of this experimental result has recently been questioned,[8] on the basis of a theoretical analysis of possible isotope effects and of reported kinetic data for both 1,2-d_2 and 1-^{13}C-

(1) Rabinovitch, B. S.; Schlag, E. W.; Wiberg, K. B. *J. Chem. Phys.* **1958**, *28*, 504-505.

(2) Berson, J. A.; Pedersen, L. D. *J. Am. Chem. Soc.* **1975**, *97*, 238-240. Berson, J. A.; Pedersen, L. A.; Carpenter, B. K. *J. Am. Chem. Soc.* **1976**, *98*, 122-143.

(3) Berson, J. A. *Annu. Rev. Phys. Chem.* **1977**, *28*, 111-132. Berson, J. A. In *Rearrangements in Ground and Excited States*; de Mayo, P., Ed.; Academic Press: New York, 1980; Vol I, pp 311-390. Borden, W. T. *Reactive Intermediates*; Wiley: New York, 1981; Vol. II, Chapter 5. Dervan, P. B.; Dougherty, D. A. In *Diradicals*; Borden, W. T., Ed.; Wiley: New York, 1982; pp 107-149. Carpenter, B. K. *Determination of Organic Reaction Mechanisms*: Wiley: New York, 1984; pp 62-67.

(4) Yamaguchi, Y.; Schaefer, H. F., III; Baldwin, J. E. *Chem. Phys. Lett.* **1991**, *185*, 143-150.

(5) Setser, D. W.; Rabinovitch, B. S. *J. Am. Chem. Soc.* **1964**, *86*, 564-574.

(6) Cianciosi, S. J.; Ragunathan, N.; Freedman, T. B.; Nafie, L. A.; Baldwin, J. E. *J. Am. Chem. Soc.* **1990**, *112*, 8204-8206.

(7) Cianciosi, S. J.; Ragunathan, N.; Freedman, T. B.; Nafie, L. A.; Lewis, D. K.; Glenar, D. A.; Baldwin, J. E. *J. Am. Chem. Soc.* **1991**, *113*, 1864-1866.

(8) Getty, S. J.; Davidson, E. R.; Borden, W. T. *J. Am. Chem. Soc.* **1992**, *114*, 2085-2093.

0002-7863/92/1514-9401$03.00/0